China Active Faults Database and its Web System

Xiyan Wu[1], Xiwei Xu[2, 3], Guihua Yu[1], Junjie Ren[3], Xiaoping Yang[1], Guihua Chen[1], Chong Xu[3], Keping Du[4], Xiongnan Huang[1], Haibo Yang[1], Kang Li[3], Haijian Hao[1]

[1] State Key Laboratory of Earthquake Dynamics, Institute of Geology, China Earthquake Administration, Beijing 100029, China
[2] School of Earth Sciences and Resources, China University of Geosciences, Beijing 100083, China
[3] National Institute of Natural Hazards, Ministry of Emergency Management of China, Beijing, 100085, China
[4] Beijing Normal University, Beijing100091, China

Correspondence to: Xiwei Xu (xiweixu@vip.sina.com)

Abstract. Active faults are potential destructive earthquake sources and also the most serious strips of earthquake disasters in the future. Studies and investigations of active faults are necessary for earthquake hazard reduction. This study presents a nation-scale database of the active faults ~~for~~ China and its adjacent regions in tandem with an associated web-based query system. This database is an updated version of the active faults data included in the "Seismotectonic Map of China and its Adjacent Regions (1:4 000 000)," which is one of the four essential maps of the mandatory Chinese standard GB/T 18306-2015 Seismic Ground Motion Parameter Zonation Maps of China. The data update and integration are based on ~~the latest 20-year region-scale~~ active fault ~~survey data~~ (1:250 000 – 1:50 000). Those data include geophysical probing, drill logging, offset-landform measuring, and sample dating, as well as geometric and kinematic parameters of exposed and blind faults, paleo-earthquake sequences, and recurrence intervals, and have been obtained and analyzed using the same technical standard framework and reviewed by expert panels in the field and laboratory. The database can be interrogated using a Web Geographic Information System (GIS) application, which provides browsing, inquiring, analyzing, and downloading functions on a web browser. The system also publishes the Open Geospatial Consortium (OGC) Web Feature Service and OGC Web Map Service of active fault data. Users can add map layers and download fault data in the OGC-compliant GIS software for further analyses via these services. The Chinese government, research institutions, and companies have widely used the active faults data from the previous versions of the Database. The database is available at https://doi.org/10.12031/activefault.china.400.2023.db (Xu, 2023) and via the Web System (CEFIS (V2), 2023; CAFD WFS). ~~It is downloadable through diverse platforms and clients as introduced in Sections 4.3.2 and 4.4.~~

1 Introduction

Earthquake is one of the most dangerous natural disasters in the world. A ~~close~~ relationship exists between large or great earthquakes and ~~the spatial distribution of an~~ active fault. In general, an earthquake of magnitude (M) ≥ 7.0 often occurs on

active faults or overlaps with them. In statistics， almost all M≥ 8.0 earthquakes and most M=7.0–7.9 earthquakes in China have been associated with rupture parts of the main boundary fault around the Tibetan Plateau block in western China and Ordos block in Central and East China (Xu and Deng, 1996; Deng et al., 2003; Zhang et al., 2003; Xu et al., 2016a). Furthermore, more than 70 co-seismic surface rupture zones generated by the great earthquakes are spatially coincident with the known active faults (Xu and Deng, 1996; Zhang et al., 2003; Xu et al., 2017). Therefore, determining the geometries and locations of the active faults and their slip rates, and then constructing a corresponding database of the active faults is essential for preventing and mitigating social and economic losses caused by destructive earthquakes and protecting lives and property (Xu et al., 2002, 2006; Tian et al., 2006).

Some countries have constructed comprehensive active faults databases in the past twenty years (Haller et al., 2004; Basili et al., 2008, 2021; Yoshioka and Miyamoto, 2011; Ganas et al., 2013; Langridge et al., 2016; Emre et al., 2018, Maldonado et al., 2021; Williams et al., 2022), some of which are publicly available. For example, the National Institute of Geophysics and Volcanology of Italy published the Database of Individual Seismogenic Source (DISS) in the 2000s. The latest version of DISS is 3.3.0 (Valensise and Pantatosti, 2001; Basili et al., 2008, 2021). This latest database includes ~200 faults. The U.S. Geological Survey established the first nationwide compilation of the U.S. Quaternary Faults and Folds Database in the early 2000s, which contained ~2000 faults (Haller et al., 2004).

China is in the convergence zone of the Indian, Eurasian, and Pacific Plates where many seismogenic active faults have developed, and becomes one of the countries with the most severe earthquake disasters at present and also in history. An active faults database of China is essential for the in-depth studies of regional crustal kinematic characteristics, intraplate earthquake features, and earthquake disaster mitigation action programmes. The China Earthquake Administration built a 1:4 000 000-scale active tectonic database (Qu, 2008) in the 2000s. This database was based on Deng's 1:4,000,000-scale active tectonic map and included more than 800 active faults and 48 active folds (Deng et al., 2002, 2007). It summarized researches on active faults carried out in China before 2002 AD. However, many active faults were not thoroughly identified or studied at that time. In the following years, several field surveys have been performed to investigate the active neotectonic and seismic activities of the Circum-Pacific and Himalayan-Mediterranean seismic zones in China. To determine the accurate position and slip age of active fault, which is of capable generating destructive earthquakes, a series of active fault surveys and mapping projects (Yang et al., 2018a, 2018b, 2020; Huang et al., 2021a, 2021b; Lei et al., 2008; Chai et al., 2011, Xu et al., 2015.) has been launched since 2007 in China. These projects consist of the following: 1) fundamental maps and data collection for national earthquake hazards prevention, such as the 5th generation "Seismic ground motion parameters zonation map of China" (China mandatory standard GB/T 18306-2015); 2) active fault prospecting in urban regions and their earthquake risk assessments, such as "Urban active fault experimental prospecting" (2001–2003)(Pan et al., 2002; Wang et al., 2002) and "Seismo-active-fault prospecting technology system in China" (2004–2008) (Wang et al., 2004; Deng et al., 2007;); 3) seismo-active-fault survey and mapping, such as "The Himalayan Plan: active fault mapping at scale of 1:50 000 in the north China tectonic region and along the North-South seismic zone" and "Earthquake risk assessment of active faults in the key earthquake surveillance and prevention areas"; 4) other scientific researches. Accurate geometric and

activity kinematic parameters as well as mechanical properties for the studied active faults are identified in those projects by systematically analyzing the published scientific literature, remote sensing data, field surveys, and dating samples from geological profiles, trenches and boreholes (Xu et al., 2015). A professional panel then reviewed the obtained parameters and rechecked the final results to ensure reliability. In every project, an overall prospecting-and-surveying-process database is built to record all project data from beginning to end. Those project databases include data associated with the geophysical prospecting, drilling, offset-landform measuring and age dating (e.g., cosmogenic nuclides, OSL, ESR, or ^{14}C used for dating offset-landform, and OSL or ^{14}C used for dating dislocated-strata in trench), geometric and kinematic parameters of the exposed and blind faults, paleo-earthquakes, their occurrence ages and recurrence intervals. The data types include two-dimensional Geographic Information System (GIS) data, photographs, geological photos with interpretated faults and illustrations , geophysical prospecting data, electronic literature with copyright, and scientific reports. By the end of 2019, the project's total amount of data reached 7 Terabytes.

The China Active Faults Database (CAFD) is a comprehensive geospatial database that summarizes the most reliable results of the abovementioned projects, based on two basic databases with accuracy of 1:50,000 single active fault mappings and 1:250,000 regional active fault distribution. The web-based query system is open to the public and shares the latest version of China's active fault database (CEFIS (V2)). Section 2 introduces the history and development of nationwide active fault maps and databases in China. Data acquisition, data resources, data processing, database compilation, and data quality are discussed in Section 3. In addition, several classical application cases in Section 3.9 are presented to demonstrate the extensive use of the database. The construction, function, performance, and usage of the web-based active fault query system are described in Section 4. System users can browse and query fault information, obtain data from the Web Feature Service (WFS) and Web Map Service (WMS) servers in GIS software (such as ArcGIS and QGIS), and add active faults as layers in their web applications.

2 Nationwide active fault maps and databases

Different organizations and experts compiled the nationwide active tectonics and fault maps of China during different periods. Every map summarized all of the research as much as possible before its publication date. Those maps, such as the "Spatial distribution map of active tectonics and strong earthquakes in China (1:3 000 000)" (NEIZMT, 1976), "Map of the major tectonic-system activity and strong earthquakes epicenter distribution in China (1:6 000 000)" (NEIZMT, 1978), "Seismotectonic map of China (1:4 000 000)" (GICEA, 1979), and "Lithospheric dynamics map of China and adjacent sea area (1:4 000 000)" (Ma, 1987), had systematically summarized the latest research achievements at specific periods.

In the past ten years, the most influential nationwide active fault maps have been "The Active Tectonic Map of China (1:4 000 000)" (Deng et al., 2007) and "Seismotectonic Map in China and its Adjacent Regions (1:4 000 000)" (SMCAR; Xu et al., 2016). Deng et al. (2007) has been widely shared with scientists, specialists, and the public over the past 10 years, although not available online. Its earlier version was integrated into the early version of Active Faults of Eurasia Database

(Trifonov et al., 2004), of which an updated version was published in 2022 (Zelenin et al., 2022). Currently, the database can be freely downloaded online (NEDC (sub-center in IG, CEA), 2023), and scientists have updated this map based on new findings. For example, Wu et al. (2018) compiled a "spatial distribution map of active faults in China and its adjacent sea areas (1:5 000 000) (2018)" by synthesizing past decadal publications in Chinese and English and 15-year research on active faults achieved by the Institute of Geomechanics in the Chinese Academy of Geological Sciences.

The SMCAR (Xu et al., 2016) is a subproject of the 5th generation "Seismic ground motion parameter zonation maps of China" and one of the four essential maps of the Chinese mandatory standard GB/T 18306-2015. This standard aims to develop seismic fortification criteria for anti-earthquake design in different regions. The SMCAR collected the latest re-activation ages of faults from the previously introduced nationwide maps and some public or unpublic data. The SMCAR is now open to the public on the web system of the 5th generation "Seismic ground motion parameter zonation maps" (GB18306, 2023), and has a geospatial database edition in addition to print and Joint Photographic Experts Group editions. This database integrates seismically active faults in China and adjacent regions and is also known as CAFD (2015). After geospatial correlation by remote sensing images in the WGS84 coordinate system, its spatial accuracy was better than that of previous congeneric maps and data. The fault data included the fault attributes of the name, main character, and faulting age. A simplified version is applied to construct a probabilistic seismic hazard model for Mainland China (Rong et al., 2020).

3 Latest version of China Active Faults Database

3.1 Active faults database compilation workflow

The CAFD (2022) presented in this paper, which is based on the most reliable results of the projects introduced in Section 1, is an updated version of the CAFD (2015). The compilation workflow of the database is illustrated in Fig. 1.

The data used to update the nationwide CAFD (2015) are obtained from 120 regional project databases and research on active fault surveys, earthquake surface rupture investigations, and published literature in the past 20 years. The 120 regional project databases are obtained and produced under the same technological system based on well-established knowledge of active fault surveys (Sections 3.2-3.4) and meet the technical demands of the Chinese mandatory standard (GB/T 36072-2018). Every regional project database uses the same data schema and standard recommended by the China Earthquake Administration (GB/T 36072-2018; DB/T 53-2013; DB/T 65-2016; DB/T 81-2020; DB/T 82-2020; DB/T 83-2020). All parameter values of the fault data are calculated using the same systematic criteria and definitions (Section 3.7). As the data definition, schema, and acquisition method are the same, there is no information gap between these project databases. All data are processed using the same workflow. First, multiple-scale active fault data are extracted from different databases. Second, they are used to update the geometric shapes and attributes of the corresponding fault data in a nationwide database. Finally, the updated database (2022) is translated into English, adjusted for deployment, and released online (Sections 3.4 and 3.6).

The CAFD (2022) is obtained from numerous surveys (Section 3.5) and research ~~references~~ (Xu et al., 2008a, 2008b, 2009a, 2009b; Chen et al., 2009; Xu et al., 2014a, 2014b; Xu et al., 2000; He et al., 2013; Shu et al., 2016, 2020; Li et al., 2019). It reflects the current state of the integrated knowledge based on seismically active fault surveys in China.

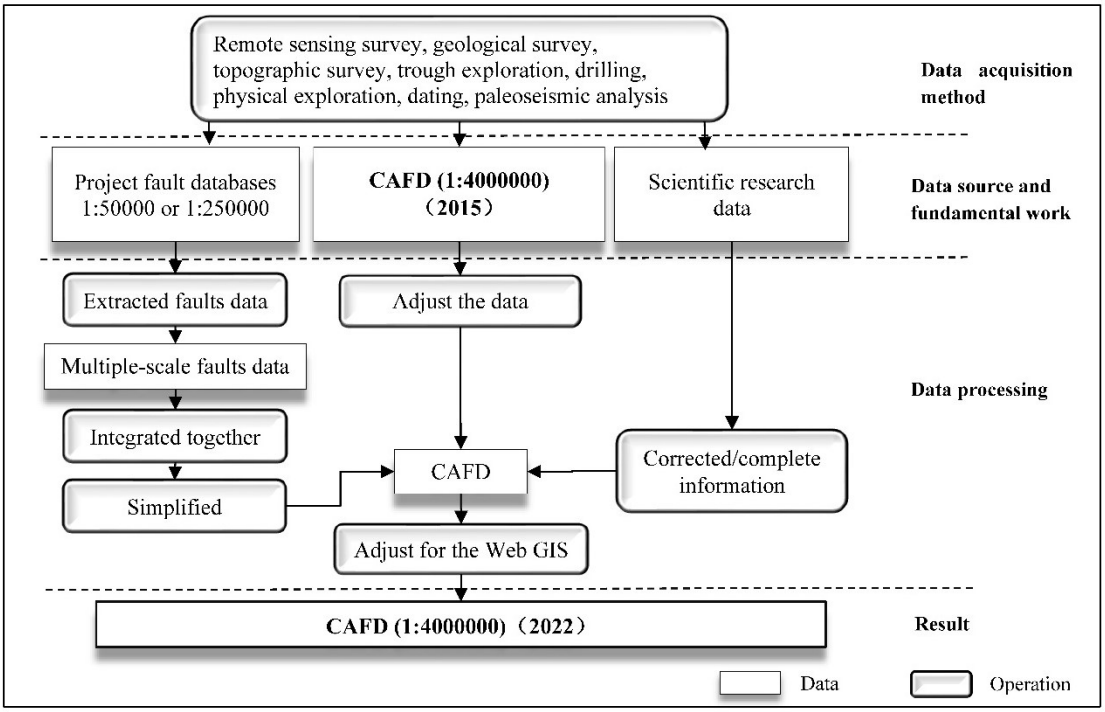

Figure 1: Workflow to construct the China Active Faults Database

3.2 Overview of data acquisition and methods

Location, geometric, and kinematic parameters of the faults stored in the nationwide CAFD (2015)(1: 1:4,000,000) (Xu et al., 2016) and regional survey project databases (1:250 000–1:50 000) are obtained through remote sensing data interpretation, geological field surveys, trenching, drilling, geophysical prospecting, dating, and paleo-seismic analysis. However, the nationwide CAFD (2015) had different accuracies from the regional survey project databases. The horizontal accuracy of the nationwide database on the scale of 1:4,000,000 is about 12.8 kilometers (GB/T 33178-2016). The nationwide CAFD (2015) (Xu et al., 2016) is based on previous studies. In earlier research, the low-resolution seismic petroleum exploration profiles caused the low accuracy of the interpreted top breakpoints. Because of that, the accuracy of positional precision of the blind faults was not precise. The locator devices with a low positioning accuracy limited the accuracy of positional precision of the exposed faults. The observation sites had a lower density than currently because of less funding, thereby causing a low positional accuracy. The horizontal accuracy of survey mapping projects on a scale of 1:50000 is 37.5 meters. (GB/T 33177-2016), and the urban active fault survey projects on 1:250000 is 200 meters (GB/T 33178-2016). The regional fault survey

project databases (1:250 000–1:50 000) are based on quantitative methods written into the Chinese mandatory standard in 2018 (GB/T 36072-2018). These were classified as the exposed fault survey method (Section 3.3) and blind survey method (Section 3.4), and guaranteed a better data quality and accuracy than the nationwide CAFD (2015) (Xu et al., 2016).

3.3 Exposed fault survey method

The exposed faults refer to the faults having surface expressions (such as linear fault scarp, offset gullies, and folding) or fault outcrop. In the present-day fault database, we only strengthen the locations, motion mode, and ages of these near-surface faults. The fault geometry or dipping angle as suggested by seismic data was not included. For the exposed faults with surface traces, remote sensing and DEM (Digital Elevation Model) data are used first to map the fault traces and create an initial distribution map of the active faults. Then, combined with the field surveys, the locations of the faults in this initial map are verified, corrected, and recorded. Finally, a systematic method that combines geomorphological surveys, stratigraphic analyses of the geological cross sections, trench stratigraphic logs, sample dating from terraces and trenches, and paleo-earthquake identification are used to obtain the latest faulting ages and kinematic parameters of the mapped active faults (DB/T 53-2013; Chen et al., 2016; Sun et al., 2017; Shi et al., 2019, 2022; Guo et al., 2021; Huang et al., 2021a).In this systematic method, the dislocated strata, samples, and trenches are accurately located in typical offset landforms. The number of paleo-earthquake events and the motion mode of faults are visualized in the trenches. The age of fault activity is determined by the ages of dislocated strata, measured by dating methods, including radiocarbon (^{14}C), cosmogenic nuclides (^{10}Be), and luminescence techniques.

Taking the Fodongmiao–Hongyazi Fault, which is mapped at a scale of 1:50 000 (Yang et al., 2018a, 2018b, 2020; Huang et al., 2021a, 2021b), as an example for the quantitative technical demands in the Chinese mandatory standard (GB/T 36072-2018). First, remote sensing images with meter-level resolution (Quickbird, worldview, SPOT, and so on) and DEMs with horizontal and relative vertical resolutions of $\leqslant$ 37.5 m (SPOT, and so on) were used to mark surface deformations or offset landforms (fault scarps, dislocated gullies, fault valleys, pull-apart basins, pressure ridges, terraces, alluvial or fluvial fans and so on) and plan geological survey sites, lines, and areas. Following these marks and positions, the fault could be traced along the fault strike, and the coordinates of the exposed fault site are precisely recorded by using Global Navigation Satellite System and hand-held GPS receiver. The average interval of coordinate-recording sites is 500–2 000 m, but if the surveyor was able to access a site, an interval of 500 m is required (Fig. 2; DB/T 53-2013). The density of the recorded sites controls the geometric accuracy of the fault data. The horizontal location error of every recorded site was less than 15 m. If the surface deformations or offset landforms disappear in some areas, the approximate fault location should be taken from the original interpretation of the high-resolution remote sensing images and DEM data. Subsequently, the next exposed fault segment is searched by traveling across the region in a "Z" route. When the next fault segment is identified again, the fault should be traced along its strike. After these steps, the geometry of the fault trace is finally confirmed on the map. Once the fault trace is ascertained, the fault is separated into segments based on the geological landforms, geometric structure (straight, curved, bent, etc.), displacement distribution, seismic rupture characteristics, or signs of fault activity, so that each section is

relative independent. Along the key segments, typical offset landforms should be selected for further geomorphic and topographic measurements (Fig. 3a & c). In every independent segment, dislocated strata, samples, and trenches are accurately located, and the number of paleo-earthquake events is visualized in the trenches (Fig. 3b and d). The ages of dislocated strata are measured by dating methods. Common dating methods include radiocarbon (^{14}C), cosmogenic nuclides (^{10}Be), and luminescence techniques. The fault is separated into segments based on the mapped geometry. The ages obtained from a single geometry segment presented the age of this segment. It determined the latest active age of the fault, although may not be the rupture behavior. ~~They are used to identify whether or not a fault is active, to calculate its slip rate during a certain period, to determine when a paleo-earthquake occurred, the paleo-earthquake recurrence interval, and the elapsed time of the last earthquake of the corresponding fault segment~~.

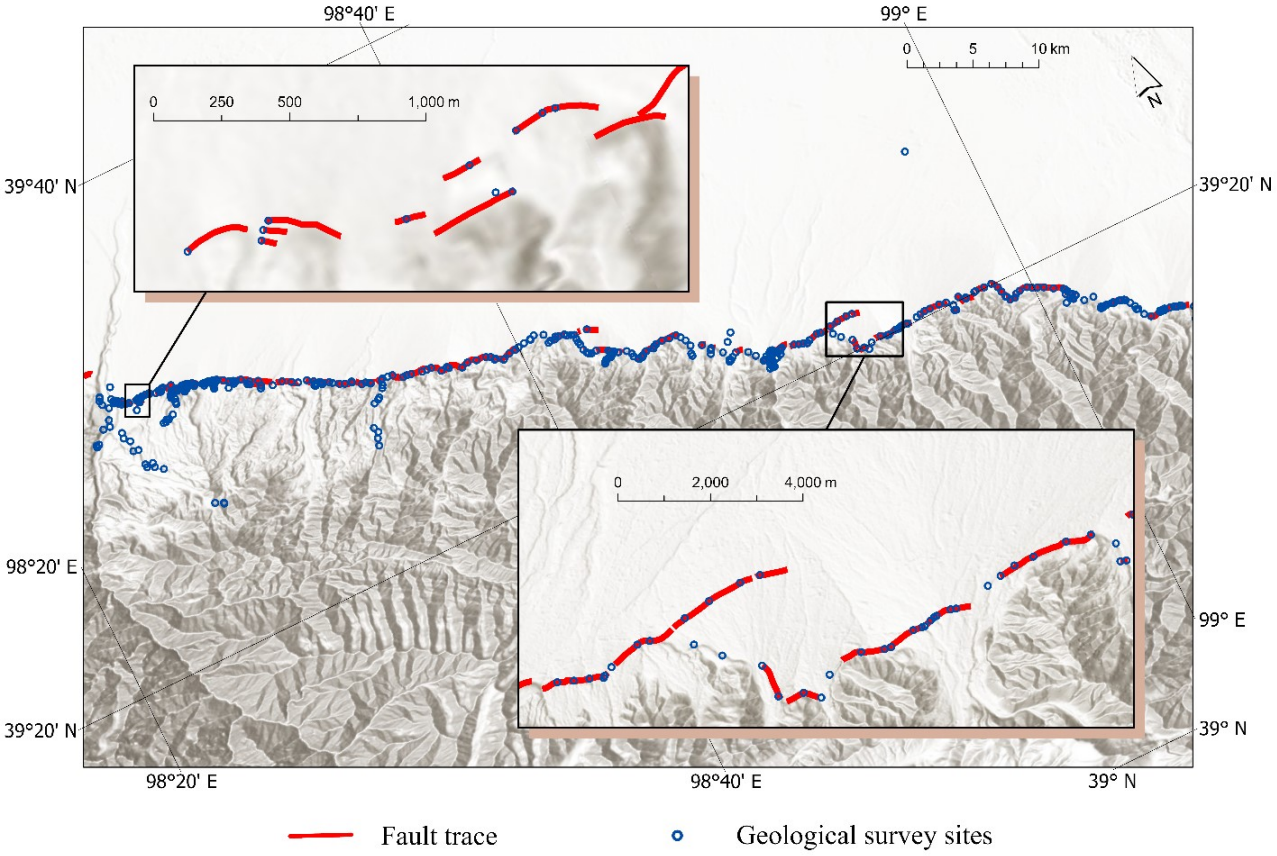

Figure 2: Survey sites for mapping of the Fodongmiao–Hongyazi Fault. The average interval of coordinate-recording sites ranges from 500–2 000 m. The fault belongs to the Qilianshan thrust fault zone at the northeastern margin of the Tibetan Plateau.

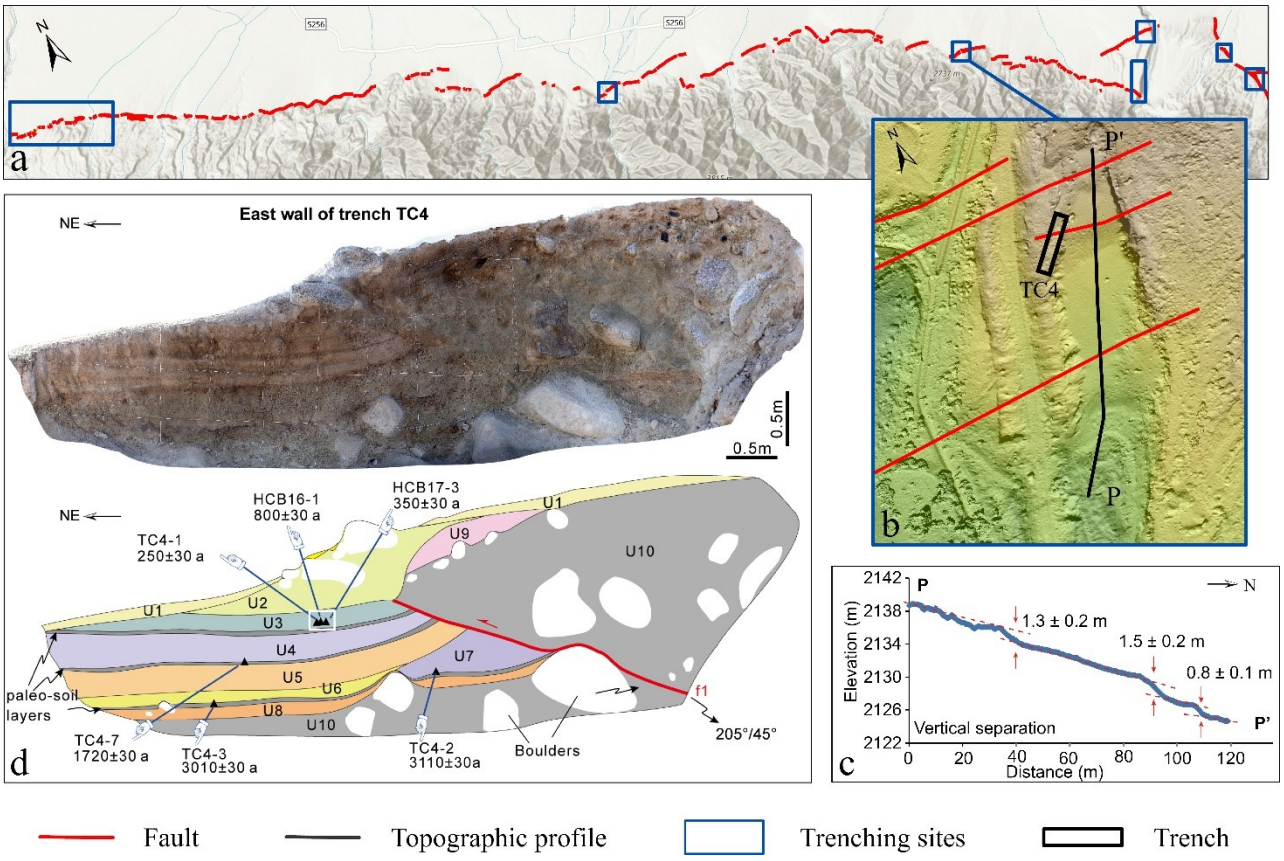

Figure 3: Key fault segment surveying example from the Fodongmiao–Hongyazi Fault (red line). (a) Distribution of the key fault segments in which geomorphic measuring, trenching, sample collecting, and paleo-earthquake trenching sites are marked by dark blue rectangles; (b) Locations of trench TC4 and topographic profile P-P′ are represented by black rectangle and black line, respectively; (c) Topographic profile (P-P′) showing fault offsets (adapted from Huang et al., 2021b); (d) Interpretation of the east wall of trench TC4 in detail (adapted from Huang et al., 2021b).

3.4 Blind fault survey method

The buried faults are those that don't cut to the near surface, have no surface expression, and are possibly covered by the overlying sediments or rocks. Firstly, we collected petroleum exploration profiles, historical earthquakes, and published references. The location of the blind faults was inferred from the collected petroleum exploration profiles. Secondly, the historical earthquakes and published references about tectonic settings helped to figure out the faults associated with earthquakes. Thirdly, a comprehensive multi-level exploration method with geophysics and drilling sites near the collected petroleum exploration profiles was applied to determine its exact near-surface location and the position of the uppermost displaced point of the major blind fault. Then samples obtained by drilling and dating techniques of the displaced and un-displaced strata and their dated chronological ages were used to identify their late Quaternary activity. This method consists of multi-level seismic exploration, joint drilling to construct a fault-across geologic section, trenching, and other technologies to detect the blind active faults from deep to shallow or even directly to the surface.

In this study, the blind Yinchuan active fault is used as an example (Fig. 4; Chai et al. 2006, 2011; Liu et al. 2008) to describe the quantitative technical demands in the Chinese mandatory standard (GB/T 36072-2018). Firstly, the seismic petroleum exploration profiles are used to reveal the approximate location of the target fault at a depth of hundreds of meters and the bottom of the Quaternary, marked by the shallowest continuous seismic reflection layer. Based on this information, a set of shallow seismic exploration profiles (in an interval of ≤ 2.5 km) is set up on the approximate ground to detect the depth of the uppermost point of the target fault. Secondly, two boreholes are drilled on both sides of the detected target fault to preliminarily verify the existence of the target faults (Fig. 5). During this exploration phase, the borehole number is gradually increased on both sides of the target fault to locate the depth of the uppermost points of the faults (Fig. 6; Chai et al., 2006; Lei et al., 2008; Wang et al., 2016). It requires at least 3 boreholes on each fault wall, with an interval of 5–45 m. The distance between the two boreholes on both sides of the target fault should be less than 10 m. Also, at least one borehole is required to penetrate the bottom of the Upper Pleistocene on each side, and the final depth of other boreholes is needed to be 10 m beneath the uppermost points determined by the shallow seismic exploration (GB/T 18306-2018). The exact location and faulting age of the target blind fault could be identified by strategic analysis and sample dating of the borehole cores. If the depth of the uppermost points determined by the joint drillings is less than 10 m deep from the ground, more information on the blind fault geometry and paleo-earthquakes could be revealed by trenching. The mapped blind fault trace is a line of vertically projected uppermost points on the ground, which are obtained by the comprehensive multi-level exploration method.

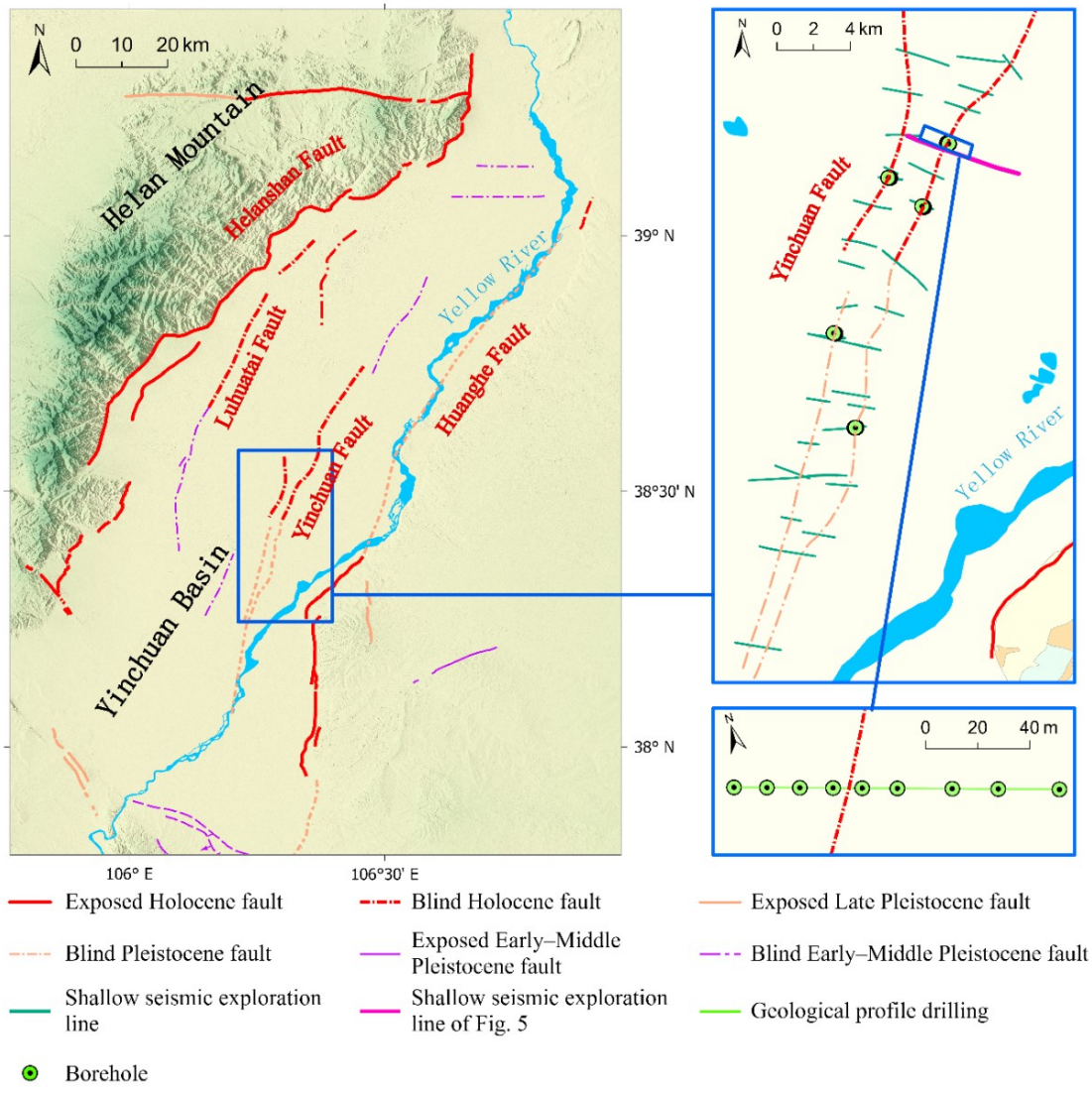

Figure 4: Map of the blind Yinchuan Fault in the Yinchuan Basin located in the northern portion of the North-South seismic zone in China.

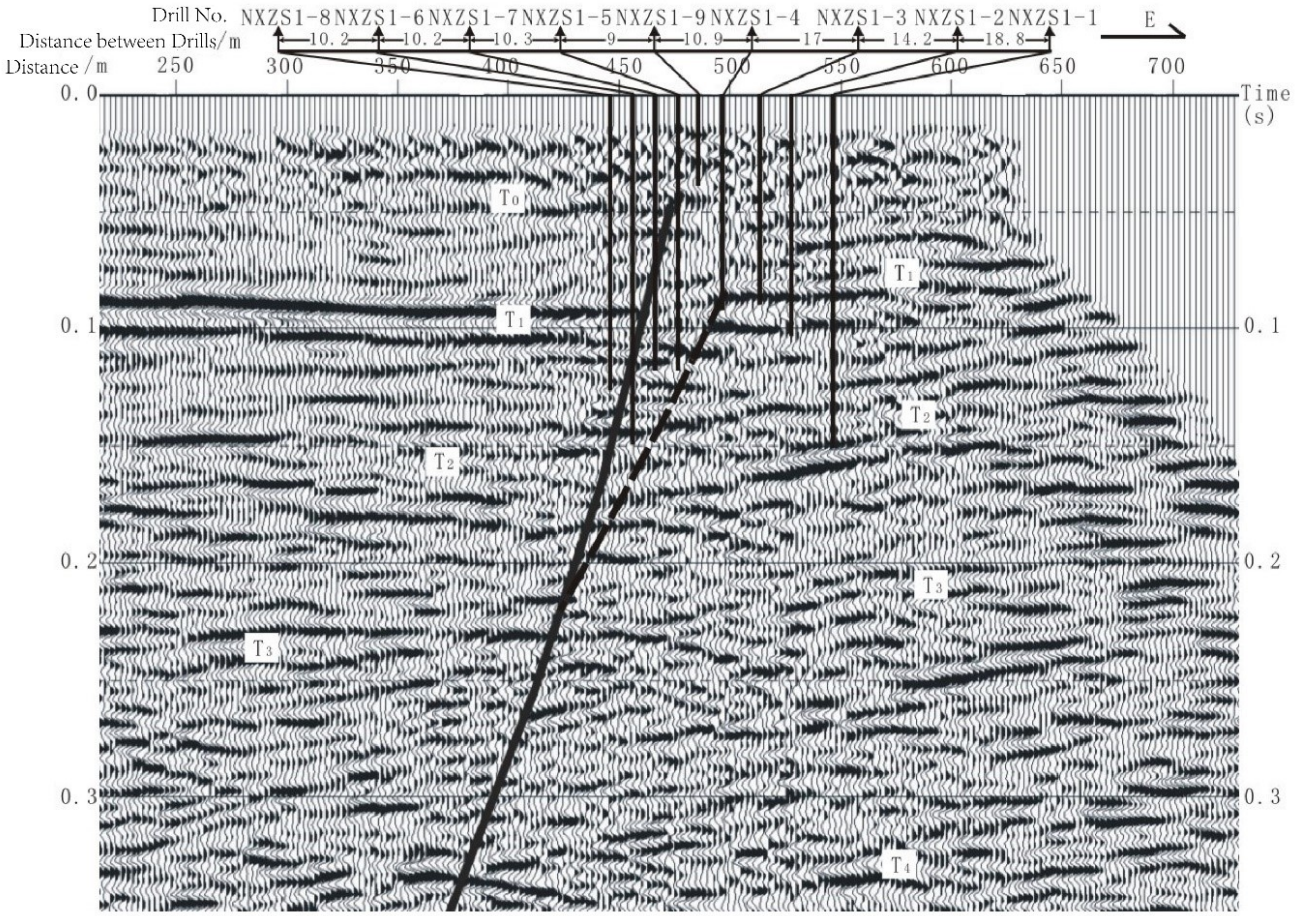

Figure 5: Approximate locations of the detected target fault and boreholes along a seismic exploration profile (adapted from Chai et al., 2011, Xu et al., 2015).

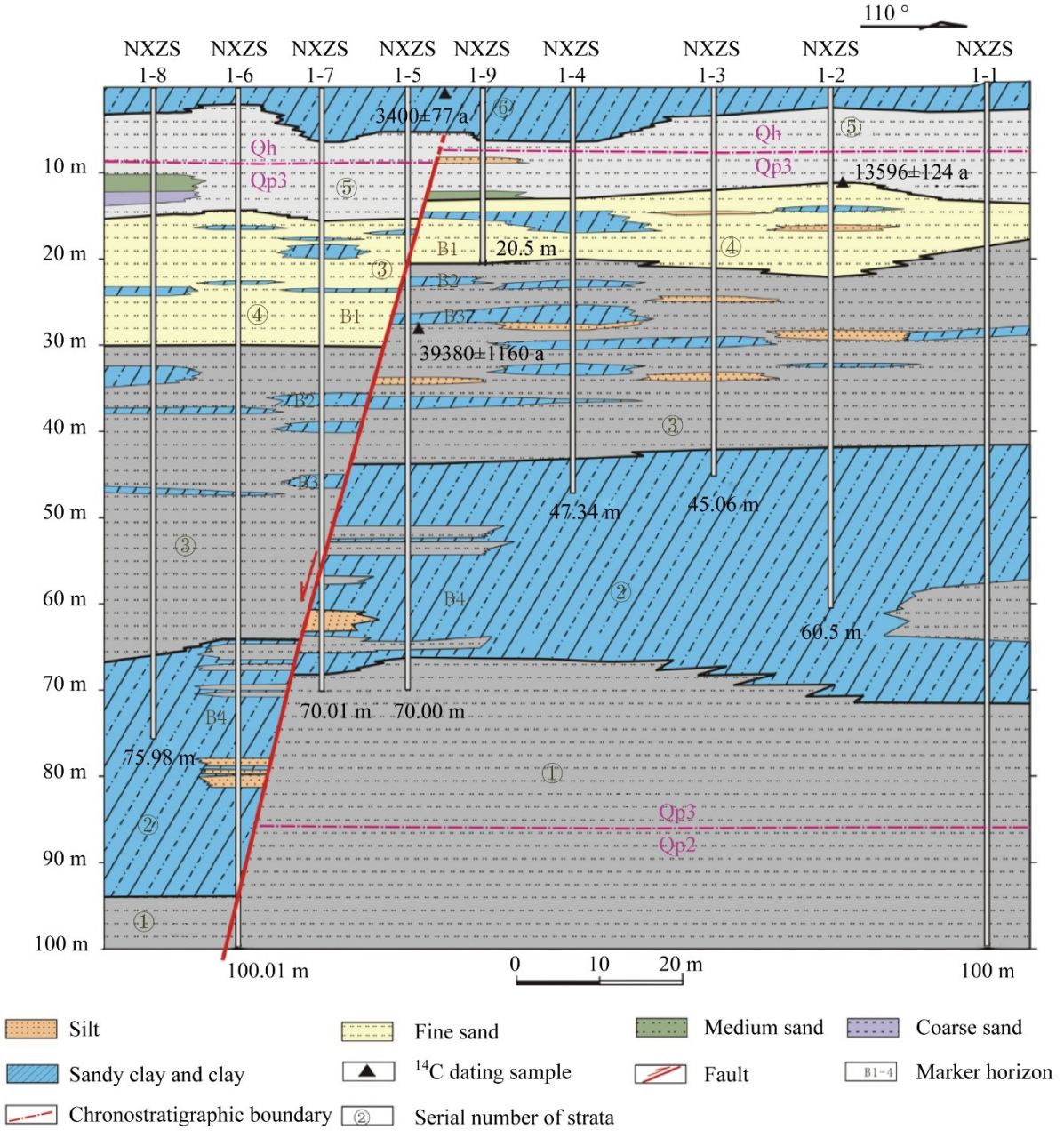

Figure 6: Joint Drilling geological cross-section at Xinqushao Village in the Yinchuan Basin (adapted from Lei et al., 2008; Chai et al., 2011).

3.5 Data sources and fundamental works

The CAFD (2022) was updated by integrating new data from the projects of active fault surveying in urban regions, seismically active fault mapping at a scale of 1:50 000 in North China and North-South seismic zone, and seismic risk assessment of the active faults in the key earthquake surveillance and prevention areas, and other scientific research (Fig. 7). These projects are introduced in detail below:

The projects of active fault surveying and seismic risk assessing focus on locating the blind or exposed seismically active faults and assessing the earthquake risk in large- and medium-sized cities and in the key earthquake surveillance and prevention areas, while the project of active fault mapping on locating such exposed seismically active faults in detail for land-use planning and utilization (Xu et al., 2015; Zhu et al., 2005; Chai et al., 2011; Liang et al., 2013; Shen et al., 2016; Hou et al., 2012; Chen et al., 2013; Yang et al., 2010). The fundamental works of these projects mainly include five parts: (1) initially identifying fault activity, (2) detecting deep structures of the fault in the crust, (3) assessing earthquake risk possibility for the identified major faults to judge seismically active faults, (4) locating the detailed geometry of the major seismically active faults, and (5) evaluation of earthquake hazards on the seismically active faults. Achievements of these projects include maps, which demonstrate the regional distribution of the active faults at a scale of 1:250 000 and detailed fault traces of a single active fault at a scale of 1:50 000, exploration reports, project databases, and information systems (Xu et al., 2015). All of the data obtained from the fundamental works and the project achievements are carefully reviewed by three to eight experts from a professional panel. Therefore, the data results were credible. These projects have been carried out in ~100 cities, including 26 provincial capitals and municipalities, until March 2020. Twenty urban active fault survey project databases (Table A1), which were conducted from 2002 to 2009 in Beijing, Tianjin, Shanghai, Nanjing, Ningbo, Zhengzhou, Qingdao, Hohhot, Taiyuan, Xi'an, Yinchuan, Lanzhou, Xining, Lhasa, Kunming, Urumqi, Haikou, Guangzhou, Changchun, and Shenyang (Fig. 7), are earliest fault data published and released to the public (Xu et al., 2015), and are also used to update the nationwide active fault database.

Active fault survey and mapping projects on scales of 1：50 000 and 1:250 000 are funded by China Earthquake Administration. The goal is to obtain the exact location, spatial distribution, geometric and kinematic parameters, activity age, slip rate, paleo-earthquake events and their recurrence intervals, and the elapsed time of the last surface-rupturing event on the faults. These projects followed the procedure introduced in Sections 3.2-3.4 and meet the quantitative requirements of mandatory and recommended standards (GB/T 36072-2018; DB/T 53-2013; DB/T 65-2016; DB/T 81-2020; DB/T 82-2020; DB/T 83-2020). A professional panel reviewed the field data and mapping results to guarantee data quality. In this study, ~100 mapped faults (Fig. 7) in North China, the North-South seismic zone, and the Tianshan region are selected to update the nationwide active fault database (Table A2).

The focus of scientific research projects has been placed on answering specific scientific questions about active faults and earthquakes. In those projects, seismo-tectonics and seismo-genesis at some sites or in some regions are studied based on the fault's geometric and kinematic features. The results are credible and provide parameters such as reliable slip rates, paleo-

earthquake sequences, the potential magnitude of future earthquakes, coseismic slips, and their distribution along the strike of a seismogenic active fault. To update the nationwide active fault database in this study, data from the 2021 M7.4 Madoi Earthquake investigation (Chen et al., 2022), 2008 M 8.0 Wenchuan Earthquake investigation (Xu et al., 2008a, 2008b, 2009a, 2009b; Chen et al., 2009), 2014 M 6.5 Ludian Earthquake investigation (Xu et al., 2014a, 2014b), Xia-Dian Fault survey (Xu et al., 2000; He et al., 2013), and research on the Tanlu Fault (Shu et al., 2016, 2020; Li et al., 2019) were used (Fig. 7).

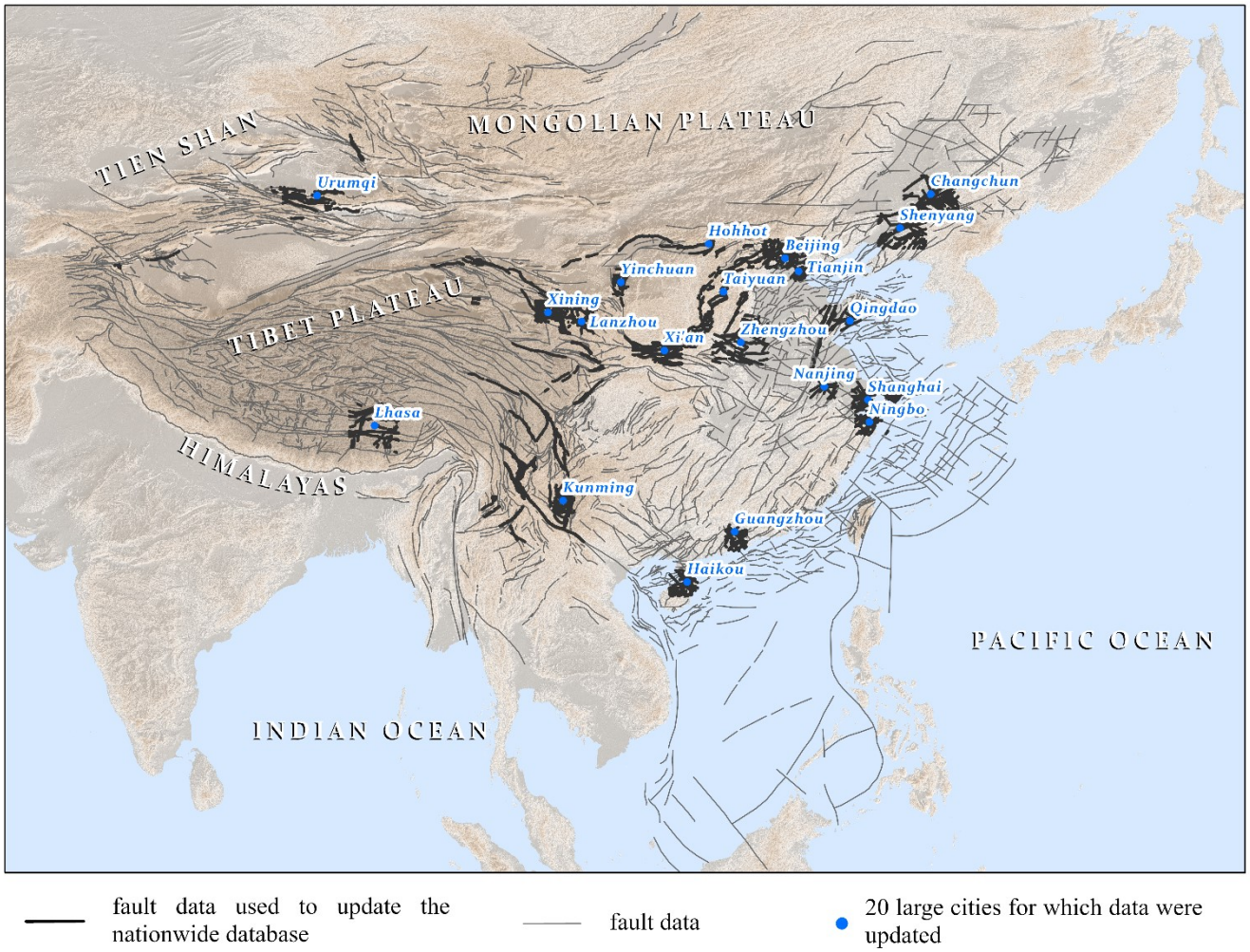

Figure 7: Sketch map of updated fault data in China.

3.6 Data processing

The CAFD (2015), project databases of active fault surveys and mappings in different regions and the scientific research data have been established. The data are complex, with multiple scales and accuracies, and the total data size is large. As

introduced in Section 1, the databases of active fault surveys and mappings include 115 sub-databases with a total size of ~7 Terabytes of data. All data are supervised and reviewed by professional panels to ensure they are all highly accurate and reliable. For the primary purpose of introducing the newest integrated achievements in this study, the reliability of fault data is not individually described. To integrate those large datasets into a unified database with the same data criteria and schema, we first integrated those project databases constructed on a regional scale and then updated the national-scale CAFD (Fig. 1). Major updates of the 1:4 000 000 nationwide database include the activity ages and locations of the late Pleistocene and Holocene faults.

The project databases of active fault surveys and seismically active fault mappings are constructed by using the same criteria. They have the same data schema and use unified, well-established acquisition methods. Therefore, the fault data from these two types of databases can be processed using the same procedures, with a small workload for data cleaning and mining. The first step involves extracting multi-scale fault data from the 120 project databases. The second step is to integrate them. These projects are systematically planned so that, theoretically, fault data with the same scale do not overlap. If the same region contains more than one fault trace, only the largest-scale data are used for integration. As the scales of the new well-mapped fault traces are equal to or even larger than 1:250 000, they are too complex to be integrated into 1:4 000 000-scale data. Therefore, the third step is to simplify the fault traces. In large-scale fault data, a fault is generally segmented for detailed investigation; hence contiguous segments may have different activity ages. One of the most important applications of the database is hardcopy or electronic image maps for earthquake emergency response (Wu, et al., 2021). The reference scale of the hardcopy maps is about 1:4 000 000~1:1 000 000. If the contiguous segments within 2 cm have different activity ages, they will be merged for map generalization. When integrated into the national scale fault data, two or even more small contiguous segments may be merged into one. Under this condition, the activity age of the merged fault trace is the same as the latest of the merged segments. For example, the blind Yinchuan fault (1:250 000) is divided into the Holocene north segment (Fig. 4a, red dotted line in the blue rectangle) and the late Pleistocene south segment (Fig. 4a, orange dotted line in the blue rectangle). The total length of those two segments is 80 km, which is only 2 cm on a 1:4 000 000 scale map. Therefore, the two segments are merged into a Holocene one.

Scientific research has mainly focused on one segment or a limited number of surveying sites for one fault. Those data are used to supplement the CAFD (2022), to complete and correct the national-scale fault data using a similar method. The CAFD (2015) was based on the same data definition and acquisition methods previously described, but its data schema slightly differs from the project databases of the fault surveys and mappings concerning field names and domain values. Considering that the CAFD (2015) has fewer fault traces than the project databases, we adjust the CAFD schema to fit the project databases. Subsequently, the processed data introduced in the previous two paragraphs are smoothly integrated into the CAFD (2022). The CAFD (2022) is adjusted for deployment in the Web-GIS system before being published in the last step.

3.7 Data descriptor

The active fault database is translated into English before being deployed in the system and released so scientists and engineers could use it worldwide. Its fields include the fault zone name, fault name, fault segment name, kinematic features, and activity age (Table A3).

The fault data are graded based on size and characteristics using the fields of fault zone name, fault name, and fault segment name. A fault zone is a large fault system such as the Tanlu and Longmenshan fault systems. In general, faults in the same system matched in geometry and kinematics, together with accumulated crustal strains, or possibly connected in deep. A single-fault system consists of several faults. A single fault is divided into multiple segments. Each segment has specific and different geometric and kinematic characteristics and is a basic studied unit of a fault. Each fault line data point belongs to one fault segment. Not all faults belong to a fault system.

Only some important active fault line data belonging to a fault system in block boundary zone have a “fault zone name”. Some highly studied faults are divided into segments and the corresponding fault line data have “fault segment names.” Because of the complications and massive number of faults in China, rating and naming must be continued.

The field named “feature” stores the motion type and visibility from the fault on the ground. Based on the relative movement of the two walls, the faults were classified as normal, reverse, strike-slip, or oblique faults. Oblique faults consist of left- and right-oblique slip faults, with vertical components that might be either normal or reverse. Active faults are also divided into exposed and buried faults.

The active fault database is aimed at earthquake hazard reduction and focuses on the latest activity during the Quaternary. Therefore, faults are classified as the Holocene, late Pleistocene, middle–early Pleistocene and pre-Quaternary faults, denoted by the field “Age” (GB/T 36072-2018). The Holocene faults are those with active evidence from the Holocene or the past 12 000 years. For the late Pleistocene faults, active evidence exists in the late Pleistocene but not in the Holocene. The middle–early Pleistocene faults are those with the latest active evidence in the middle or early Pleistocene. For pre-Quaternary faults, active evidence is not available in the Quaternary. This means that no evidence showed that the fault displaced the Quatenary landforms or sediments. There was also no Quaternary fault age information such as the ESR dating fault gouge. Major active evidence is based on the latest dislocated stratum. This method is introduced in Sections 3.3-3.4.

3.8 Quality discussion

The CAFD (2022) collects the maximum amount of reliable data relative to earthquakes with the primary objective of effectively reducing earthquake hazards by determining earthquake sources and carrying out active tectonic zonation. It performs well in terms of quantity and quality. The spatial correlation between faults and earthquakes with magnitudes greater than 6.5 is high. The amount of fault data is large. The database contains ~7 000 fault traces， among which 1 606 faults are named. The fault names were collected from published or unpublished papers, geological literature, or existing

fault databases. There are two naming methods. One is named after the mountains and rivers. The other is named after the place name (county, village, etc.).

Active fault surveys in China are difficult because the country is located in the intersection region of the Circum-Pacific and Eurasian seismic zones, resulting in complex continental tectonics, widely distributed active faults, strong neotectonics and earthquake activities, and inaccessible landforms. The extent of seismo-genic fault research varies from region to region in China. For some faults with low research extent, their geometric and kinematic parameters remain unknown or imprecise. In the periphery and interior of the Tibetan Plateau, which was formed during the colliding between the Indian and Eurasian Plates, there exist mega-strike-slip fault systems, such as the Altyn Tagh, east Kunlun and Xianshuihe Faults, the thrust fault systems, e. g. the Himalayan frontal, Hexi Corridor and Longmenshan thrusts, and the North-South striking normal faults in the western Plateau. The thrusts and strike-slip fault have also been developed at the northern and southern piedmonts and in its interior. In some regions in the Tianshan and Tibetan Plateau due to the high altitude and snow-capped, it is difficult to carry out research work and obtain accurate fault data. There exist numerous oblique normal faults around the Ordos Block and strike-slip faults, such as the Tanlu fault in Eastern China. Those faults are located in regions with dense urban construction and populations or thick quaternary deposits. Therefore, it is difficult to find those fault traces on the ground and locate the blind faults underground. Besides, the spatial relationship and geometrical link of some faults, such as some segments of the Tanlu fault in Eastern China and some E-W trending faults in the Tibetan Plateau, also remain unclear.

Thus, the vector lines of such faults directly cross each other without expressing a geometrical link. In addition, research on marine and maritime island faults has been limited by surveying technology.

As the Active Fault Database in China is based on 1:4 000 000 data and was updated by 1:250 000–1:50 000 data, the total coordinate accuracy is similar to the 1:1 000 000 map in which 1 mm is equal to 1 km in the real world and represents the width of the fault line symbol. The data precision is partially better than that of the 1:1 000 000 map because the reference is on a larger scale.

Based on the discussion above, the CAFD (2022) is based on the latest research on active faults and fault data integration. More investigations of active tectonics and fault systems should be carried out in China, and the nationwide database should be updated in the future.

3.9 Application

The CAFD (2022) and its previous versions have been widely used by the Chinese government, research institutions, and associated companies. The National Geomatics Center of China and the China Petroleum & Chemical Corporation take those data as reference data to analyze the seismotectonic environment for their information management systems. The national-scale Active Faults Database is the basic reference for compiling seismotectonic maps on a regional or national scale. Examples include the seismotectonic map of the Ordos block and its boundary zones (1:500 000; National Research and Development Program of China; No. 2017YFC150100), digital seismotectonic map of the northeastern seismic zone in China (1:1 000 000; a Spark Plan project funded by the China Earthquake Administration; No. XH18015), seismotectonic

map of the Shanxi Province and its adjacent regions (1:500 000; a public service map produced by the Shanxi Earthquake Agency), and seismotectonic map of China (1:1 000 000; first comprehensive natural hazard risk investigation in China). They are also used in earthquake emergency response services, monitoring services, forecasting services, and earthquake disaster prevention supervised by the China Earthquake Administration. The database has been delivered to the earthquake response departments of the China Earthquake Networks Center for emergency actions since 2018. In 2018, it was also delivered to the working research group of the post-earthquake prediction technology system, a key project in earthquake monitoring and forecasting from the China Earthquake Administration (Project No. 18440680117). In 2019, this database was transferred to the China Earthquake Disaster Prevention Center to establish the Data Center for Seismic Active Fault Surveys. The Institute of Geology, China Earthquake Administration (IG, CEA), has also produced seismotectonic maps during earthquake emergencies based on the database (Wu et al., 2021). As the system discussed in this study was released online, a commercial app (GeoQuater) became available that uses the WFS service of this database as a thematic map. The WFS service is stable on the application.

4 System Introduction

4.1 System performance and architecture

The China Earthquake and Fault Information System (CEFIS(V1), 2021), which has been launched online and updated since 2019, provides web services for inquiring about earthquakes and active faults in China and adjacent regions. The CAFD (2015) has been released in the system. In 2021, the system was updated again by simplifying the interface, adding the English fields, earthquake base map, layer addition, and system sharing function. A simplified case of a regional active fault survey map (Wu et al., 2022), introduced in Sec 3.3, is also open to the public as a map service in the additional layer list. This section introduces the architecture of the URL's current version (CEFIS (V2), 2023).

The system is constructed on ArcGIS Enterprise platform 10.6 using ArcGIS Web AppBuilder in the B/S mode and is separated into four layers (Fig. 8) namely data, service, portal, and application layers.

The data layer deploys the PostgreSQL database to store active fault and earthquake data. PostgreSQL is a free open-source object-relational database system that can be connected to an ArcGIS Server deployed in the service layer. The ArcGIS Server can publish data in the form of map and feature services, which can be conveniently called web applications. The ArcGIS Portal and ArcGIS Web Adaptor are deployed in the portal layer to provide WMS and WFS services and manage user access. The ArcGIS Portal provides intuitive what-you-see-is-what-you-get applications such as AppBuilder with ready-to-use widgets. These applications are used to construct a map and three-dimensional scene applications on the web. The system in this study is also constructed using ArcGIS Web AppBuilder. Supported by these technologies, the CAFD can be accessed on various platforms through desktop software, smartphones, and online sites.

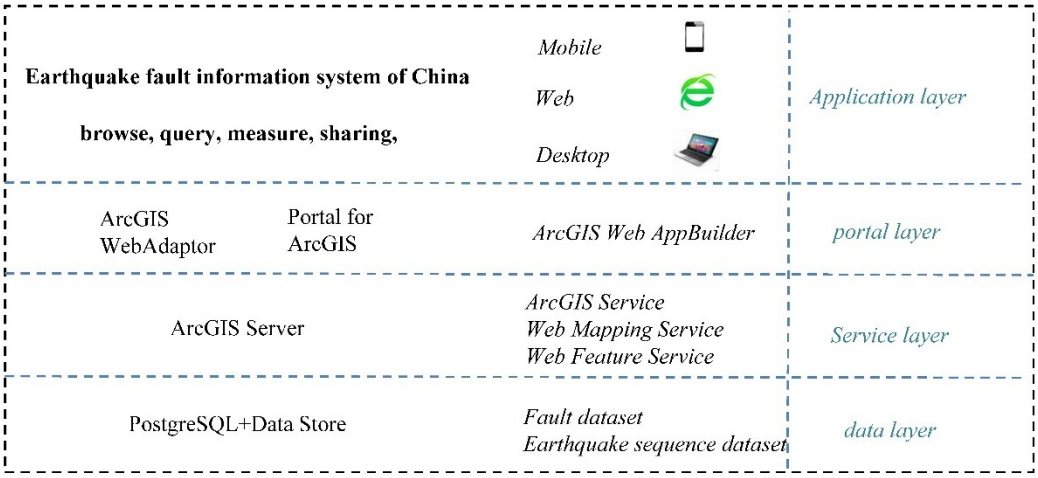

Figure 8: System architecture diagram.

4.2 Earthquake sequence data

The system uses earthquakes (M > 5.0) as a background to show earthquake activity on and around faults. The earthquake catalog from the National Earthquake Data Center (NEDC) is converted into geographic vector data and deployed in the system (Earthquake sequence data from NEDC, 2023). It contains historical and instrumental records of earthquakes that occurred before June 2021. The system contains three earthquake layers. Those correspond to the three datasets downloaded from the NEDC. The NEDC provides three datasets based on the following periods: a historic earthquake catalog (before ~1969.12.31.; Table A4), the earthquake catalog of the China Earthquake Networks (CEN; 1970.1.1.-2008.12.31.; Table A5), and the official earthquake catalog from the CEN (2009.1.1.-2023.7.31.; Table A6). The historic earthquake catalog compiled by Gu (1983) includes destructive earthquakes (M ≥ 5.0) that occurred from 1831 BC to 1969 AD. The CEN earthquake catalog consists of data from 88 National seismograph network stations (digital), regional someone-on-duty network stations (digital), and simulated network stations. The official earthquake catalog is from CEN, which is obtained from nationwide earthquake monitoring station networks consisting of national and regional (31) station networks after January 1, 2009.

4.3 System using

4.3.1 System interface and function

The system is a Web Map application that displays and queries the Active Faults Database of China and its adjacent regions. It is publicly available worldwide. The system interface consists of seven parts (Fig. 9): (a) web map, (b) eagle-eye map, (c) attribute table, (d) browsing tools, (e) address geolocation tool and (f & g) system tools.

The language of the system interface is based on the browser's default language. The data field values are in both English and Simplified Chinese in the attribute table and Query dialogue. Thus, the system can be used by both English and Chinese users.

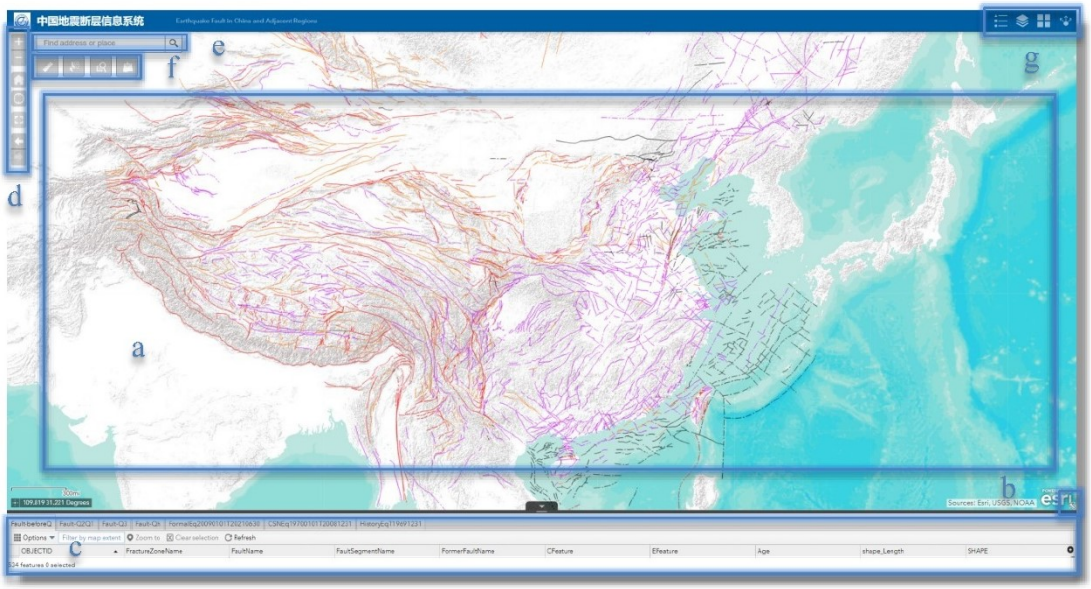

Figure 9: System interface. (a) Web map displaying only fault traces in full extent view; when zoomed into the regional scale, earthquake epicenters will appear on the map. (b) Accordion overview map. (c) Accordion attribute table. (d) Navigation toolbar; the tools from top to bottom are zoom in, zoom out, default extent, zoom to the current position, full extent, previous view, and next view. (e) Address geolocation tool. System tools: (f) measurement, selection, inquiry, and layer addition (from left to right) and (g) legend, layer controller, base maps, and sharing (from left to right).

4.3.2 Data query and export

The system provides four methods for querying fault information: (1) The menu of the attribute table window (Fig. 9a) provides a "filter" tool to query faults with certain conditions (Fig. 10a); (2) the second tool is a spatial selection tool (Fig. 9f) for fault and earthquake data (Fig. 10c); (3) the third tool allows fault queries by feature, activity age, or name under specific spatial conditions (Figs. 10b and 9f); (4) the address geolocation tool (Fig. 9e) can be used to zoom the map into a specific region and export the faults in that region (Fig. 10d). The system can export the query results using diverse methods (Fig. 10).

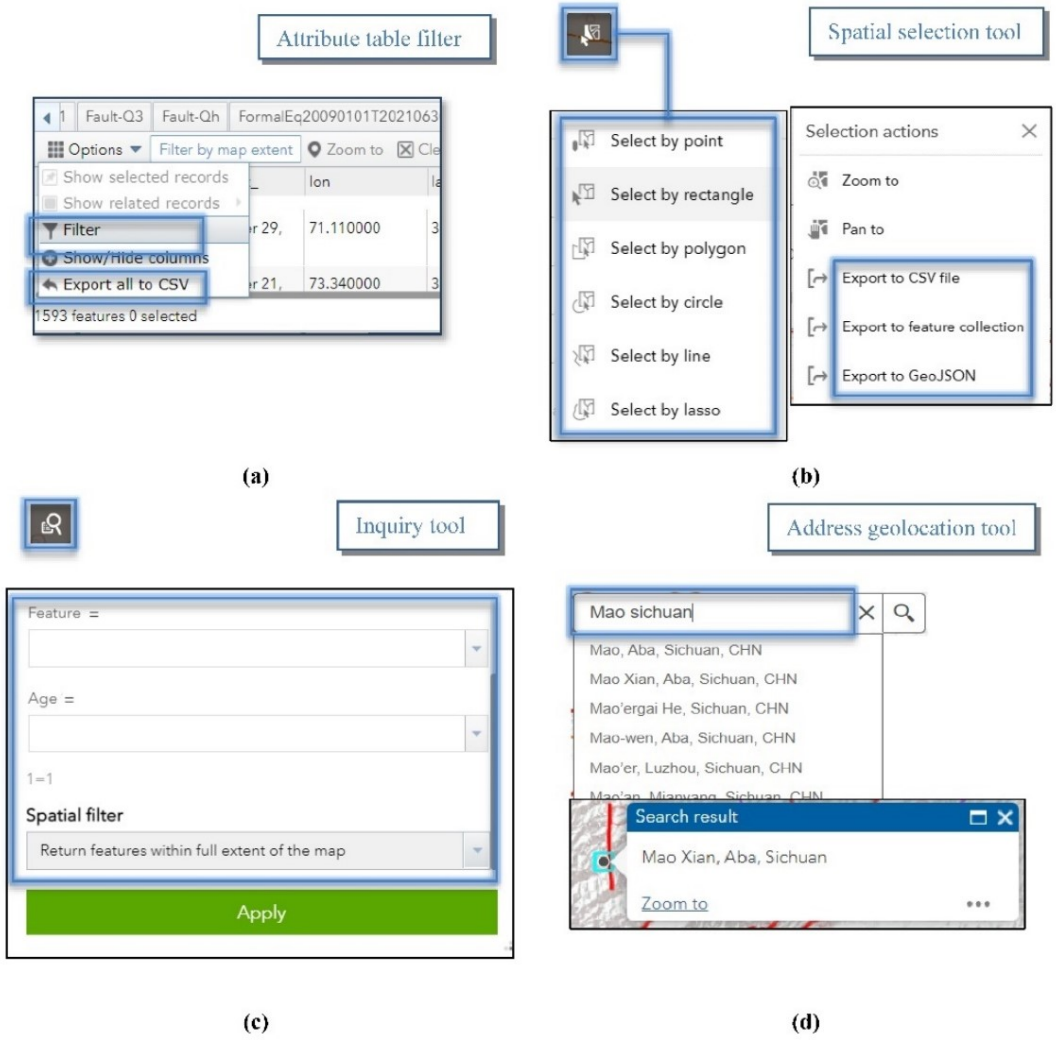

Figure 10: Data query and export tools: (a) attribute table filter, (b) spatial selection tool, (c) inquiry tool, and (d) address geolocation tool (translated by Google Chrome).

4.4 How to use the data service

The system publishes the Open Geospatial Consortium (OGC) WFS and WMS of the active fault database of China. The OGC WFS and WMS are dynamic services that provide dynamic maps on the web, following the specifications of the OGC. These services allow web maps to access diverse platforms and clients openly and authentically. Available operations of the WMS in the system in this study are GetCapabilities, GetLegendGraphic, GetSchemaExtension, GetFeatureInfo, and GetMapGetStyles. Compared with WMS, WFS provides greater data access, benefiting from its ability to insert, update, delete, retrieve, and discover geographic elements over HTTP in a distributed environment. Available WFS operations are GetCapabilities, DescribeFeatureType, GetPropertyValue, GetFeature, GetGmlObject, ListStoredQueries, and

DescribeStoredQueries. In other words, data can be browsed, queried, analyzed, and downloaded from the system, but not revised. Fault layers can also be added to GIS software for analysis through WMS and WFS such as ArcGIS Pro and QGIS (Fig. 11).

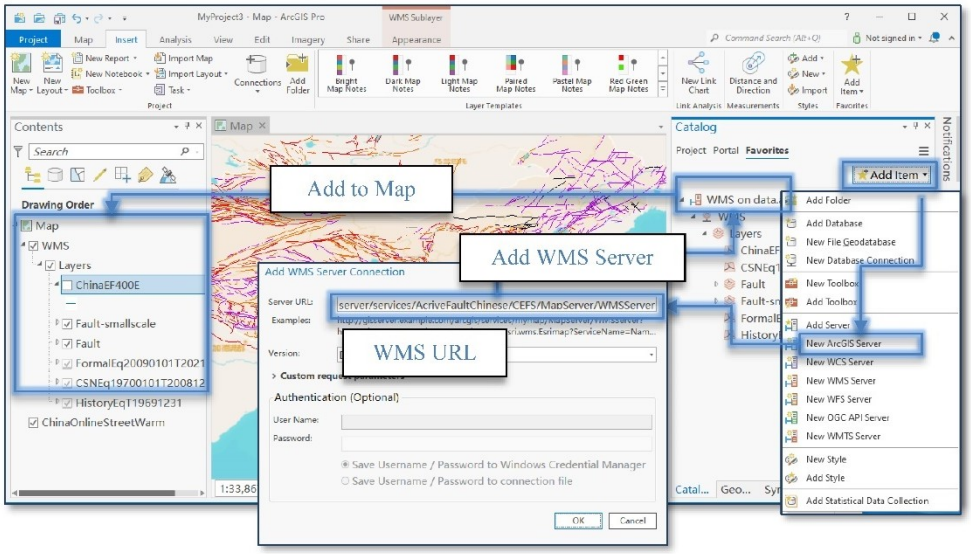

(a)

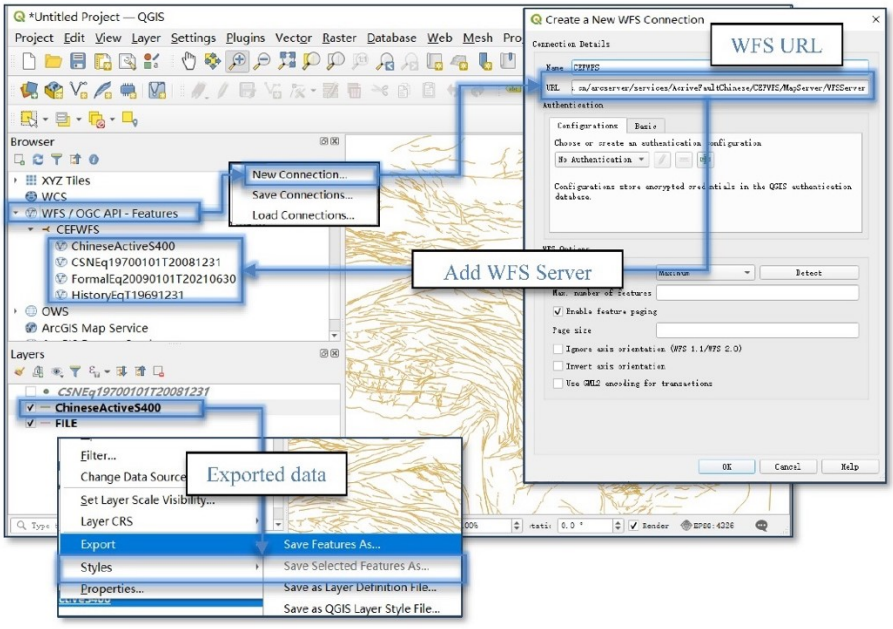

(b)

Figure 11: (a) How to add WMS Server in ArcGIS Pro. (b) How to add WFS Server in QGIS and export data.

5 Conclusions

The CAFD (2022) is integrated with the national-scale fault database and the latest decadal regional-scale fault survey data and represents the most complete nationwide seismo-active fault data in China. The database and its previous versions have been widely applied in government departments, research institutes, and commercial companies. China is situated in the intersection between the Circum-Pacific and Eurasian seismic zones with numerous complex continental tectonics, active faults, and earthquake activity. However, it is difficult to survey or locate active faults in some regions due to inaccessible landforms and anthropogenic activities. Active faults should be considered for earthquake prevention and mitigation. Therefore, the database will be gradually updated in the future based on future references, and a later version may be released on the system if it is finished.

The first version of the web system (CEFIS (V1), 2021) has operated well for nearly 2 years and its second version (CEFIS (V2), 2023) was released in 2021 and has also been operating well. This study introduces its architecture, interface, function, and usage to provide a platform to query and analyze the integrated active faults database in China, which stores the location, latest activity age, and geometric and kinematic characteristics of the faults. Although the interface environment is in the Chinese language, English-speaking users can also use the system introduced in Section 4.3.

Data and services are openly shared worldwide via the web system. The data can be downloaded from a browser or GIS software. A third-party application can link to and use the WMS and WFS services (CAFD WMS, 2023; CAFD WFS, 2023). Users can get help from the ArcGIS online document. Section 4.4 lists the available operations of the services.

6 Data availability

The CAFD and web system are accessible at CEFS (V2) under the DOI: https://doi.org/10.12031/activefault.china.400.2022.db (Xu, 2022). The WMS (CAFD WMS, 2023) and WFS (CAFD WFS, 2023) services of the active fault are accessible online. The data are downloadable through diverse platforms and clients as introduced in Sections 4.3.2 and 4.4. The Earthquake catalogs are downloaded from the Data Sharing Infrastructure of the National Earthquake Data Center (http://data.earthquake.cn) The data are not freely downloadable. Their information and links are below. FormalEq20090101T20210630:
https://data.earthquake.cn/datashare/report.shtml?PAGEID=datasourcelist&dt=40280d0453e414e40153e44861dd0003
CSNEq19700101T20081231:
https://data.earthquake.cn/datashare/report.shtml?PAGEID=datasourcelist&dt=40280d0453e414e40153e44861dd0002
HistoryEqT19691231:
https://data.earthquake.cn/datashare/report.shtml?PAGEID=datasourcelist&dt=8a85efd754e7d6910154e7d691810000

510

7 Appendix A

515 **Table A1: Cities list for updating the CAFD**

No.	City Name	Work Content	Reference Scale
1	Beijing	UAFS	1:250000
2	Haikou	UAFS	1:250000
3	Huhehaote	UAFS	1:250000
4	Kunming	UAFS	1:250000
5	Lasa	UAFS	1:250000
6	Nanjing	UAFS	1:250000
7	Ningbo	UAFS	1:250000
8	Qingdao	UAFS	1:250000
9	Shanghai	UAFS	1:250000
10	Shenyang	UAFS	1:250000
11	Taiyuan	UAFS	1:250000
12	Xian	UAFS	1:250000
13	Changchun	UAFS	1:250000
14	Zhengzhou	UAFS	1:250000
15	Wulumuqi	UAFS	1:250000
16	Xining	UAFS	1:250000
17	Guangzhou	UAFS	1:250000
18	Tianjing	UAFS	1:250000
19	Lanzhou	UAFS	1:250000
20	Yinchuan	UAFS	1:250000
UAFS: Urban Active Fault Survey			

Table A2: Faults list for updating the CAFD

No.	Fault Name	Work Content	Reference Scale
1	Xiaojiang fault	SM	1:50000
2	Junggar Basin south margin fault and Huoerguosi-Manasi-Tugulu fault	SM	1:50000
3	Laohushan fault and Maomaoshan fault	SM	1:50000
4	Tanlu fault zone	SM	1:50000
5	Xiangshan-Tianjingshan fault	SM	1:50000
6	Keketuohai-ertai fault	SM	1:50000
7	Honghe fault	SM	1:50000
8	Xianshuihe fault	SM	1:50000

9	Zemuhe fault	SM	1:50000
10	Anninghe fault	SM	1:50000
11	Langshan piedmont fault and Sertengshan Piedmont fault	SM	1:50000
12	Daqingshan piedmont fault	SM	1:50000
13	Xuanhua Basin north margin fault and Xuanhua Basin north margin fault	SM	1:50000
14	Huoshan fault	SM	1:50000
15	Taibai-Weishan piedmont fault	SM	1:50000
16	southern margin fault of Huaian basin (Western segment)	SM	1:50000
17	southern margin fault of Huaian basin (Eastern segment)	SM	1:50000
18	Heyang-Hancheng fault	SM	1:50000
19	Zhongtiaoshan piedmont fault	SM	1:50000
20	Northern margin fault of Emeitaidi	SM	1:50000
21	Luoyunshan piedmont fault	SM	1:50000
22	Taigu fault	SM	1:50000
23	northern foothill fault of the Hengshan mountains	SM	1:50000
24	Anqiu-Juxian fault	SM	1:50000
25	Yunongxi (Bawolong) fault	SM	1:50000
26	Litan fault and	SM	1:50000
27	eastern foothill fault of the Yulongxueshan Mountains	SM	1:50000
28	Weixi-Qiaohou-Weishan fault	SM	1:50000
29	Kusaihu-Maqu fault and Maqu-Heye fault	SM	1:50000
30	hanmuba-Lancang fault and Hanmuba fault	SM	1:50000
31	Shipping-Jianshui fault	SM	1:50000
32	Qujiang fault	SM	1:50000
33	Dayingjiang fault	SM	1:50000
34	Longlin-Ruili fault	SM	1:50000
35	Honghe fault (middle & Northern segment)	SM	1:50000
36	Anninghe fault	SM	1:50000
37	Xiaojiang fault South segment & North segment	SM	1:50000
38	Xianshuihe fault Moxi segment	SM	1:50000
39	Nantinghe fault	SM	1:50000
40	Xiaojiang fault	SM	1:50000
41	Yuanmou fault	SM	1:50000
42	Lijiang-Xiaojinhe fault	SM	1:50000
43	Heqing-Eryuan fault	SM	1:50000
44	Deqin-Zhongdian fault	SM	1:50000
45	Ninglang fault	SM	1:50000
46	Longpan-Qiaohou fault	SM	1:50000
47	Litang fault & Dewu fault & Labo fault & Xisasi fault	SM	1:50000
48	Daju fault	SM	1:50000
49	Chenghai fault	SM	1:50000
50	Ganzi-Yushu fault	SM	1:50000
51	Longriba fault	SM	1:50000
52	Tazang fault	SM	1:50000
53	Bailongjiang fault	SM	1:50000
54	Hanan-Qingshanwan-Mobali fault	SM	1:50000
55	Guanggaishan-Dieshan fault	SM	1:50000
56	Lintan-Dangchang fault	SM	1:50000

57	Lenglongling fault	SM	1:50000
58	Riyuanshan fault	SM	1:50000
59	Eastern foothill fault of the Liupanshan mountains	SM	1:50000
60	Guguan-Baoji fault	SM	1:50000
61	Southern margin fault of the Wuwei Basin	SM	1:50000
62	Minle-Damaying fault	SM	1:50000
63	eastern foothill fault of the Yumushan Mountains	SM	1:50000
64	Bodongmiao-Hongyazi fault	SM	1:50000
65	Yumen fault	SM	1:50000
66	Hanxia-Dahuanggou fault	SM	1:50000
67	Cangma fault	SM	1:50000
68	Eastern foothill fault of the Luoshan mountains	SM	1:50000
69	Guanguanling fault	SM	1:50000
70	TianqiaoGou-Huangyangchuan fault	SM	1:50000
71	Jintananshan fault	SM	1:50000
72	Altyn Tagh fault （Eastern segment）	SM	1:50000
73	Sertengshan Piedmont fault	SM	1:50000
74	Langshan piedmont fault	SM	1:50000
75	Yabulaishan fault	SM	1:50000
76	Jinshajiang fault	IFA	1:250000
77	Minjiang fault and Huya fault	IFA	1:50000
78	Yemahe Snow Mountain Fault Zone	SM	1:50000
79	Sanweishan fault	SM	1:50000
80	Keping fault	SM	1:50000
81	Kashi fault	SM	1:50000
82	Daliangshan fault	SM	1:50000
83	Liulengshan piedmont fault	SM	1:50000
84	Longmenshan Fault Zone (Middle segment)	SM	1:50000
85	South Tianshan fault zone	SM	1:50000
86	Southern margin fault zone of the Yuguang Basin	SM	1:50000
87	Jiaocheng fault	SM	1:50000
88	Xiadian fault	SM	1:50000
89	North margin fault of the Wulashan	SM	1:50000
90	Fukangnan fault	SM	1:50000
91	Huashan piedmont fault	SM	1:50000
92	Tomloan fault & Mingyaole fault & Kazikeaerte fault	SM	1:50000
93	Northern margin fault of the Daihai	SM	1:50000
94	Southern margin fault of the Chaiwobao Basin	SM	1:50000
95	Cixian-Daming fault	SM	1:50000
96	earthen foothill fault of the Helanshan mountains	SM	1:50000
97	Northern margin fault of the Ordos Basin	IFA	1:250000
98	Bayinhaote fault	SM	1:250000
99	Haixiu fault	IFA	1:250000
100	Southern margin fault of the Balikun Basin	SM	1:50000

SM: survey mapping. IFA: identification of fault activity.

Table A3: Attributes of fault data.

Field name	Description
FractureZoneName_Ch	(in simplified Chinese) Fracture zone name. Only some
FractureZoneName_En	(in English) Fracture zone name.
FaultName_Ch	(in simplified Chinese) Fault name.
FaultName_En	(in English) Fault name.
FaultSegmentName_Ch	(in simplified Chinese) Fault segment name.
FaultSegmentName_En	(in English) Fault segment name.
FormerFaultName	(in simplified Chinese) Former name of fault.
Feature_Ch	(in simplified Chinese) Kinetic property and detectability of the fault segment.
Feature_En	(in English) Kinetic property and detectability of the fault segment.
Age	(in English abbreviations) The active age of the fault segment.

Table A4: Attributes of HistoryEqT19691231.

Field Name	Description
time_beiji	The origin date and origin time of the earthquake (GMT +8).
lon	Epicentral longitude of the earthquake.
lat	Epicentral latitude of the earthquake.
dep	The focal depth of the earthquake is in km.
magnitude	Magnitude (M).
intensity	(Macro) epicentral intensity.

Table A5: Attributes of CSNEq19700101T20081231.

Field Name	Description
time_gmt_	The origin date and origin time of the earthquake (GMT).
lon	Epicentral longitude of the earthquake.
lat	Epicentral latitude of the earthquake.
dep_km_	The focal depth of the earthquake is in km.
ms	Surface wave magnitude.
ms7	Surface wave magnitude was computed from records of the Chinese-made long-period seismograph of type 763 (Cheng et al., 2017).
ml	Local magnitude.
mb	Body wave magnitude, measured by short-period body wave recording (mb).
mb_1	Body wave magnitude, measured by medium-period body wave recording (mB).

Table A6: Attributes of FormalEq20090101T20210630.

Field Name	Description
Date	The origin date and origin time of the earthquake (GMT +8).

lon	Epicentral longitude of the earthquake.
lat	Epicentral latitude of the earthquake.
dep_km_	The focal depth of the earthquake in km.
magnitude	Magnitude type.
magnitude	Magnitude.

Author contributions

Conceptualization, XX, and XW; Data curation, GY, XW, GC, JR, KL, and CX; Formal analysis, KD, XX, XW, GY; Funding acquisition, XX, GY, and XW; Investigation, XX, XW, GY, GC, XY, HY, and XH; Methodology, GY, XW, KD, GC, JR, KL, and CX; Project administration, XX, GY, and XW; Software, KD and XW; Supervision, XX and GY; Validation, XX and XW; Writing, XW and XX. All authors have read and agreed to the published version of the manuscript.

Competing interests

The authors declare that they have no conflict of interest.

Acknowledgments

We acknowledge all colleagues who have contributed to the active fault databases in China in the past decades. Many scientists and engineers have participated in active fault surveys and mappings and made efforts to build regional-scale project databases. Their work provided basic high-quality materials.

The Earthquake catalogs are downloaded from the Data Sharing Infrastructure of the National Earthquake Data Center (http://data.earthquake.cn). We acknowledge the data support from the "China Earthquake Networks Center, National Earthquake Data Center."

Financial support

This research work was supported by the National Natural Science Foundation of China (Grant No. 41941016) and the Research and Development Program of IG, CEA (Name: active fault data management on a cloud platform).

References

Basili R., Valensise G., Vannoli P., Burrato, P., Fracassi, U., Mariano, S., Tiberti, M. M., and Boschi, E.: The Database of Individual Seismogenic Sources (DISS), version 3: summarizing 20 years of research on Italy's earthquake geology, Tectonophysics, 453(1-4), 20-43, https://doi.org/10.1016/j.tecto.2007.04.014, 2008.

Basili R., Burrato P., De Santis G. M., Fracassi, U., Maesano, F. E., Tarabusi, G., and DISS Working Group.: Database of Individual Seismogenic Sources (DISS), Version 3.3. 0: A compilation of potential sources for earthquakes larger than M 5.5 in Italy and surrounding areas, https://doi.org/10.13127/diss3.3.0, 2021.

CEFIS (V1): http://www.neotectonics.cn/arcgis/apps/webappviewer/index.html?id=3c0d8234c1dc43eaa0bec3ea03bb00bc, last access: 27 Nov 2021.

CEFIS (V2): https://data.activetectonics.cn/arcportal/apps/webappviewer/index.html?id=684737e8849c4170bbca14447608c451, last access: 12 May 2023.

CAFD WFS: http://data.activetectonics.cn/arcserver/services/Hosted/CAFD400_2022_WFS/MapServer/WFSServer, last access: 12 May 2023.

CAFD WMS: https://data.activetectonics.cn/arcserver/services/AcriveFaultChinese/CEFSL_CE/MapServer/WMSServer, last access: 12 May 2023.

Chai, C., Meng, G., Du, P., Wang, Y., Liu, B., Shen, W., Lei, Q., Liao, H., Zhao, C., Fan, S., Zhang, X., and Xie, X.: Comprehensive multi-level exploration of buried active fault: an example of Yinchuan buried active fault, Seismology and Geology, 28(4), 536, 2006 (in Chinese).

Chen, G., Xu, X., Yu, G., An, Y., Yuan, R., Guo, T., Gao, X., Yang, H. and Tan, X.: Co-seismic slip and slip partitioning of multi-faults during the MS8.0 2008 Wenchuan earthquake, Chinese J. Geophys.-Ch., 52(5), 1384-1394, https://doi.org/10.3969/j.issn.0001-5733.2009.05.028, 2009.

Chai, C., Meng, G. and Ma, G.: Active fault survey and earthquake hazard assessment in Yinchuan, Science Press, ISBN 978-7-03-030701-9, 2011 (in Chinese).

Chen, Y.: Active fault survey and earthquake hazard assessment in Tianjin, Science Press, ISBN 978-7-03-037079-2, 2013.

Chen, G., Xu, X., Wen, X., and Chen, Y.: Late Quaternary Slip-rates and Slip Partitioning on the Southeastern Xianshuihe Fault System, Eastern Tibetan Plateau, Acta Geol. Sin.-Engl., 90(2), 537-554, https://doi.org/10.1111/1755-6724.12689, 2016.

Chen, J., Rong, Y., Harold, M., Chen, G., and Xu, X.: An Mw-Based Historical Earthquake Catalog for Mainland China, B. Seismol. Soc. Am., 107(5), 2490–2500, https://doi.org/10.1785/0120170102, 2017.

Chen, G., Li, Z., Xu X., Sun, H., Ha, G., Guo, P., Su, P., Yuan Z., Li, T.: Co-seismic surface deformation and late Quaternary accumulated displacement along the seismogenic fault of the 2021 Madoi M7.4 earthquake and their implications for regional tectonics, Chinese Journal of Geophysics, 65(8): 2984-3005, https://doi.org/10.6038/cjg2022P0873, 2022 (in Chinese).

DB/T 53-2013 Mapping of active fault in 1:50 000, recommended standard by China Earthquake Administration, 2013 (in Chinese).

DB/T 65-2016 Code of 1:50 000 active fault mapping database, recommended standard by China Earthquake Administration, 2016 (in Chinese).

DB/T 81-2020 Active fault survey-Paleoseismic trenching, recommended standard by China Earthquake Administration, 2020 (in Chinese).

DB/T 82-2020 Active fault survey-Field geological investigation, recommended standard by China Earthquake Administration, 2020 (in Chinese).

DB/T 83-2020 Active fault survey-Inspection of database, recommended standard by China Earthquake Administration, 2020 (in Chinese).

Deng, Q., Lu, Z., Yang, Z.,: Remarks on urban active faults exploration and associated activity assessment. Seismology and Geology, 29(2): 189-200, 2007 (in Chinese).

Deng, Q., Zhang, P., Ran, Y., Yang, X., Min, W., and Chu, Q.: Basic characteristics of active tectonics in China, Sci. China Ser. D., 32(1), 1020-1030, https://doi.org/10.1360/zd2002-32-12-1020, 2002 (in Chinese).

Deng, Q., Zhang, P., Ran, Y., Yang, X., Min, W., and Chu, Q.: Basic characteristics of active tectonics of China, Sci. China Ser. D., 46(4), 356-372, https://doi.org/10.1360/03yd9032, 2003 (in Chinese).

Deng, Q., Ran, Y., Yang, X., Min, W., and Chu, Q.: The active tectonic map of China (1:4 000 000), Seismological Press, ISBN 978-7-50-283051-9, 2007 (in Chinese).

Emre, Ö., Duman, T. Y., Özalp, S., Şaroğlu, F., Olgun, Ş., Elmacı, H., and Çan, T.: Active fault database of Turkey. B. Earthq. Eng., 16(8), 3229-3275, https://doi.org/10.1007/s10518-016-0041-2, 2018.

Earthquake sequence data from NEDC: https://data.earthquake.cn/gcywfl/index.html, last access: 20 Jan 2023.

GB/T 18306-2015 Seismic ground motion parameters zonation map of China, mandatory standard of China, 2015 (in Chinese).

GB/T 33177-2016 National fundamental scale maps—1:5 000 1:10 000 topographic maps, 2016 (in Chinese).

GB/T 33178-2016 National fundamental scale maps 1:250 000 1:500 000 1:1 000 000 orthophoto maps, 2016 (in Chinese).

GB/T 36072-2018 Surveying and prospecting of active fault, mandatory standard of China, 2018 (in Chinese).Ganas A., Oikonomou I. A., and Tsimi C.: NOAfaults: A digital database for active faults in Greece. B. Geol. Soc. Greece, 47(2), 518-530, 2013.

GB18306: http://www.gb18306.net/detail/50, last access: 20 Jan 2023.

Geology Institute of China Earthquake Administration (GICEA), Seismotectonic map of China (1:4 000 000), 1979 (in Chinese).

Gu, G.: Earthquake catalogue of China (from 1831 BC to 1969 AD), Science Press, ISBN 13031·2238, 1983 (in Chinese).

Guo P., Han Z., Dong S., Mao, Z., Hu, N., Gao, F., and Li, J.: Latest quaternary active faulting and paleoearthquakes on the southern segment of the Xiaojiang fault zone, SE Tibetan plateau, Lithosphere, 2021(1), https://doi.org/10.2113/2021/7866379, 2021.

Haller, K. M., Machette, M. N., Dart, R. L., and Rhea, B. S.: U.S. Quaternary fault and fold database released, Eos, Transactions American Geophysical Union85(22), 218-218, https://doi.org/10.1029/2004EO220004, 2004.

Hou, K.: Active fault survey and earthquake hazard assessment in Nanjing, Seismological Press, ISBN 978-7-50-283971-0, 2012 (in Chinese).

He, F., Bai, L., Wang, J., Liu, Y., Cai, X., Sun, Y., Zhang, L., Fang, T., and Guo, G.: Deep structure and quaternary activities of the Xiadian fault zone, Seismology and Geology, 35(3), 490-505, https://doi.org/10.3969/j.issn.0253-4967.2013.03.004, 2013.

Huang, X., Yang, X., Yang, H., Hu, Z., and Zhang, L.: Re-Evaluating the Surface Rupture and Slip Distribution of the AD 1609 M7 1/4 Hongyapu Earthquake Along the Northern Margin of the Qilian Shan, NW China: Implications for Thrust Fault Rupture Segmentation, Front. Earth Sc.-Switz, 9, 98, https://doi.org/10.3389/feart.2021.633820, 2021a.

Huang, X., Yang, H., Yang, X., Yang, H., Hu, Z., and Zhang, L.: Holocene paleoeseismology of the Fodongmiao-Hongyazi Fault along the Northern Tibetan margin (Western China) and implication to intraplate earthquake rupturing pattern, Tectonophysics, 808, 228812, https://doi.org/10.1016/j.tecto.2021.228812, 2021b.

Liu, B., Chai, C., Feng, S., Zhao, C., Yuan, H.: Seismic exploration method for buried fault and its up-breakpoint in Quaternary sediment area—An example of Yinchuan buried active fault, Chinese Journal of Geophysics, 51(5), 1475-1483, 2008 (in Chinese).

Lei, Q., Chai, C., Meng, G., Du, P., Wang, Y., Xie, X., Zhang, X.: Composite drilling section exploration of Yinchuan buried fault, Seismology and Geology, 30(1), 250-263, 2008 (in Chinese).

Liang, G. and Wu, Y.: Active fault survey and earthquake hazard assessment in Guangzhou, Science Press, ISBN 978-7-03-037757-9, 2013 (in Chinese).

Langridge, R. M., Ries, W. F., Litchfield, N. J., Villamor, P., Van Dissen, R. J., Barrell, D. J. A., Rattenburya, M. S., Herona, D. W., Haubrocka, S., Townsenda, D. B., Leea, J. M., Berrymana, K. R., Nicolc, A., Coxb S. C., Stirling, M. W.: The New Zealand active faults database. New Zeal. J. Geol. Geop., 59(1), 86-96, https://doi.org/10.1080/00288306.2015.1112818, 2016.

Li, K., Xu, X., Wei, L., Wang, Q., and Shu, P.: Evidence of long recurrence times and low slip rate along the 1668 Tancheng earthquake fault, Chin Sci Bull, 64, 1168–1178, https://doi.org/10.1360/N972018-00961, 2019.

Ma, X.: Lithospheric dynamics map of China and adjacent sea area (1:4 000 000), 1987 (in Chinese).

Maldonado, V., Contreras, M., Melnick, D.: A comprehensive database of active and potentially-active continental faults in Chile at 1: 25,000 scale. Sci. data, 8(1), 1-13, https://doi.org/10.6084/m9.figshare.13268993, 2021.

Nation-scale earthquake intensity zonation map compiling team (NEIZMT): Spatial distribution map of active tectonics and strong earthquakes in China (1:3 000 000), China Earthquake Administration, 1976 (in Chinese).

Nation-scale earthquake intensity zonation map compiling team (NEIZMT): Map of the major tectonic-system activity and strong earthquakes epicentre distribution in China (1:6 000 000), China Earthquake Administration, 1978 (in Chinese).

NEDC: https://data.earthquake.cn/zcfg/index.html, last access: 20 Jan 2023.

NEDC (sub-center in IG, CEA): http://datashare.igl.earthquake.cn/map/ActiveFault/introFault.html, last access: 20 Jan 2023.

Pan, J., Liu, B., Zhu, J., Zhang, X., Fang, S., Wang, F., Duan, Y., Xu, Z.: Comparative experiment on seismic sources in high-resolution seismic exploration for urban active faults. Seismology and Geology, 24(4): 533-541, 2002 (in Chinese).

Qu C.: Building to the active tectonic database of China, Seismology and Geology, 30 (1), 298-304, 2008 (in Chinese).

Rong, Y., M.EERI, Xu, X., Jia Cheng, J., Chen, G., Magistrale, H., M.EERI, and Shen, Z.: A probabilistic seismic hazard model for Mainland China, Earthq. Spectra, 36(1_suppl), 181-209, https://doi.org/10.1177/8755293020910754, 2020

Shen, J. and Bo, J.: Active fault survey and earthquake hazard assessment in Songyuan, Seismological Press, ISBN 978-7-5028-4731-9/P(5427), 2016 (in Chinese).

Shu, P., Fang, L., Zheng, Y., Lu, S., Pan, H., Song, F., and Li, S.: Geological Evidence and Characteristics of Activity of the Wuhe-Mingguang Section of Tancheng-Lujiang Fault Zone in Late Pleistocene, Earthquake Research in China, 30(4), 485-499, 2016.

Sun, H., He, H., Wei, Z., Shi, F. and Gao, W.: Late Quaternary paleoearthquakes along the northern segment of the Nantinghe fault on the southeastern margin of the Tibetan Plateau. J. Asian Earth Sci., 138, 258-271, https://doi.org/10.1016/j.jseaes.2017.02.023, 2017.

Shi F., He H., Gao W., Sun, H., Wei, Z., Hao, H., Zou J., Sun, W., and Su, P.: Holocene paleoearthquakes on the Tianqiaogou-Huangyangchuan fault in the northeastern boundary fault system of the Tibetan Plateau, J. Asian Earth Sci., 186, 104049, https://doi.org/10.1016/j.jseaes.2019.104049, 2019.

Shu, P., Min, W., Liu, Y., Xu, X., Li, K., Yu, Z., Yang, H., Luo, H., Wei, S., and Fang, L.: Late Quaternary paleoseismology and faulting behavior of the Yilan-Yitong fault zone and implications for seismic hazards of the Tanlu fault zone, eastern China. J. Asian Earth Sci., 201,1-18, https://doi.org/10.1016/j.jseaes.2020.104509, 2020.

Shi F., He H., Liu Y., Wei, Z., and Sun, H.: Active Tectonics of the Nantinghe Fault in Southeastern Tibetan Plateau and its Implications for Continental Collision. Front. Earth Sci., 9, 818225, https://doi.org/10.3389/feart.2021.818225, 2022.

Trifonov, V. G.: Active faults in Eurasia: general remarks, Tectonophys., 380, 123–130, https://doi.org/10.1016/j.tecto.2003.09.017， 2004.

Tian, S.: Faults Investigation and Evaluation for Seismic Safety Assessment of Nuclear Power Plants, Technology for Earthquake Disaster Prevention, 1(1), 25-30, https://doi.org/10.3969/j.issn.1673-5722.2006.01.004, 2006 (in Chinese).

Valensise, G. and Pantatosti, D., Database of potential sources for earthquakes larger than M 5.5 in Italy. Version 2.0-2001. Italy: N. p., 2001. Web.

Wang, G., Wang, J., Liu, C., Liu, W., Zhang, P., Lin, Y., Zhu, J., Huang, Z., Zhao, Z.: A trial geochemical prospecting for buried active faults in Fuzhou city. Seismology and Geology, 24(4): 593-600, 2002 (in Chinese).

Wang, Y.: Recognition of "The Working guidelines for exploration and seismic risk assessment of active faults in urban areas (on trial)". Seismology and Geology, 26(4): 559-565, 2004 (in Chinese).

Wang, Y., Meng, G., Chai, C., Liu, Q., Du, P., and Xie, X.: The accurate location methods of buried active fault exploration: an example of Luhuatai faults in Yinchuan graben, Seismology and Geology, 37(1), 256, https://doi.org/10.3969/j.issn.0253-4967.2015.20, 2016 (in Chinese).

Wu, Z., Zhou, C., Ma, X., Wang, J., Huang, X., Wu, X., Hu, M., Ha, G., and Liu, J.: Active faults map of China and adjacent sees (1:5 000 000), Geological Publishing House, 2018 (in Chinese).

Wu, X., Du, K., Yu G., Chen, G., Dong, Y., Xu, X., Chen, Z., and Xu, C.: Implementation and future challenges of seismotectonic mapping system for earthquake emergency response, In IOP Conference Series: Earth and Environmental Science, 861(5), p. 052047, 2021.

Williams, J. N., Wedmore, L. N., Scholz, C. A., Kolawole, F., Wright, L. J., Shillington, D. J., Åke Fagereng, Biggs J., Mdala H., Dulanya Z., Mphepo F., Chindandali P. R. N., Werner, M. J.: The Malawi Active Fault Database: An Onshore -

Offshore Database for Regional Assessment of Seismic Hazard and Tectonic Evolution. Geochem., Geophy., Geos., 23(5), e2022GC010425, https://doi.org/10.1029/2022GC010425, 2022.

Wu, X., Xu, C., Xu, X., Chen, G., Zhu, A., Zhang, L., Yu, G., and Du, K.: A Web-GIS hazards information system of the 2008 Wenchuan Earthquake in China, 2, 210-217, Natural Hazards Research, https://doi.org/10.1016/j.nhres.2022.03.003, 2022.

Xu, X. and Deng, Q.: Nonlinear characteristics of paleoseismicity in China. Journal of Geophysical Research: Solid Earth, 101(B3), 6209-6231, https://doi.org/10.1029/95JB01238, 1996.

Xu, X., Ji, F., Yu, G., Chen, W., Wang, F., and Jiang, W.: Reconstrction of paleoearthquake sequence using stratigraphic records from drill logs: a study at the Xiadian Fault, Seismology and Geology, 22(1), 9-19, 2000 (in Chinese).

Xu, X., Yu, G., Ma, W., Ran, Y., Chen, G., Han, Z., Zhang, L., and You, H.: Envidence and methods for determining the safety distance from the potential earthquake surface rupture on active fault, Seismology and Geology, 24(4), 470-483, 2002 (in Chinese).

Xu, X.: Active Faults, Associated Earthquake Disaster Distribution and Policy for Disaster Reduction, Technology for Earthquake Disaster Prevention, 1(1):7-14, https://doi.org/10.3969/j.issn.1673-5722.2006.01.002, 2006 (in Chinese).

Xu, Z., Ji, S., Li, H., Hou, L., Fu, X., and Cai, Z.: Uplift of the Longmenshan range and the Wenchuan earthquake, Episodes, 31, 291-301. https://doi.org/10.18814/epiiugs/2008/v31i3/002, 2008a.

Xu, X., Wen X., Ye J., Ma B., Chen, Zhou, et al, The MS 8.0 Wenchuan Earthquake surface ruptures and its seismogenic structure, Seismology and Geology, 30(3), 597-629, 2008b (in Chinese).

Xu, X., Wen, X., Yu, G., Chen, G., Klinger, Y., Hubbard, J., and Shaw, J.: Coseismic reverse- and oblique-slip surface faulting generated by the 2008 Mw 7.9 Wenchuan earthquake, China, Geology, 37(6), 515-518, https://doi.org/10.1130/G25462A.1, 2009a.

Xu, X.: Album of 5.12. Wenchuan MS 8.0 earthquake surface ruptures, China, Seismological Press, ISBN 978-7-5028-3542-2, 2009b (in Chinese).

Xu, X., Jiang, G., Yu, G., and Wu X., Zhang J., and Li X.: Discussion on seismogenic fault of the Ludian M_S 6.5 earthquake and its tectonic attribution, Chinese Journal of Geophysics, 57(9), 3060-3068, https://doi.org/10.6038/cjg20140931, 2014a (in Chinese).

Xu, C., Xu, X., Shen, L., Dou, S., Wu, S., Tian, Y., and Li, X.: Inventory of landslides triggered by the 2014 M_S 6.5 Ludian earthquake and its implications on several earthquake parameters, Seismology and Geology, 36(004), 1186-1203, https://doi.org/10.3969/j.issn.0253-4967.2014.04.020, 2014b (in Chinese).

Xu, X., Yu, G., Ran, Y., Yang, X., Zhang, L., Sun, F., Du, W., and Liu, B.: Introduction on urban active faults in China: urban active fault survey achievement in 20 large cities of China, Seismological Press, ISBN 978-7-5028-4410-3, 2015 (in Chinese).

Xu, X., Guo T., Liu S., Yu G., Chen G., Wu X.: Discussion on issues associated with setback distance from active fault. Seismology and Geology, 38(003), 477-502, https://doi.org/10.3969/j.issn.0253-4967.2016.03.001, 2016a (in Chinese).

Xu, X., Han, Z., Yang, X., Zhang, S., Yu, G., Zhou, B., Li, F., Ma, B., Chen, G., and Ran, Y.: Seismotectonic Map in China and its Adjacent Regions (1:4 000 000), Seismological Press, 2016b (in Chinese).

Xu, X., Wu, X., Yu, G., Tan X., Li, K.: Seismo-Geological Signatures for identifying M≧7.0 earthquake risk areas and their premilimary application in mainland China, Seismology and Geology, 39(002), 219-275, https://doi.org/10.3969/j.issn.0253-4967.2017.02.001, 2017 (in Chinese).

Xu, X.: China Active Fault Database, Active Fault Survey Data Centre at Institute of Geology, China Earthquake Administration [data set], https://doi.org/10.12031/activefault.china.400.2023.db, 2023.

Yang, F.: Active fault survey and earthquake hazard assessment in Changchun, Seismological Press, ISBN 978-7-5028-3695-5, 2010 (in Chinese).

Yoshioka, T., and Miyamoto, F.: Active fault database of Japan: Its construction and search system. In AGU Fall Meeting Abstracts, Vol. 2011, pp. S21A-2144, 2011.

Yang, H., Yang, X., Huang, X., Li, A., Huang, W., and Zhang, L.: New constraints on slip rates of the Fodongmiao-Hongyazi fault in the Northern Qilian Shan, NE Tibet, from the 10Be exposure dating of offset terraces, J. Asian Earth Sci., 151, 131-147, https://dx.doi.org/10.1016/j.jseaes.2017.10.034, 2018a.

Yang, H., Yang, X., Zhang, H., Huang, X., Huang, W., and Zhang, N.: Active fold deformation and crustal shortening rates of the Qilian Shan Foreland Thrust Belt, NE Tibet, since the Late Pleistocene. Tectonophysics, 742, 84-100, https://doi.org/10.1016/j.tecto.2018.05.019, 2018b.

Yang, H., Yang, X., Huang, W., Li, A., Hu, Z., Huang, X., and Yang, H.: 10Be and OSL dating of Pleistocene fluvial terraces along the Hongshuiba River: Constraints on tectonic and climatic drivers for fluvial downcutting across the NE Tibetan Plateau margin, China, Geomorphology, 348, 106884, https://doi.org/10.1016/j.geomorph.2019.106884, 2020.

Yeats, R. S., K. Sieh, C. R. Allen: The Geology of Earthquakes, Oxford: Oxford University Press, 1997.

Zelenin, E., Bachmanov, D., Garipova, S., Trifonov, V., and Kozhurin, A.: The Active Faults of Eurasia Database (AFEAD): the ontology and design behind the continental-scale dataset, Earth Syst. Sci. Data, 14, 4489–4503, https://doi.org/10.5194/essd-14-4489-2022, 2022.

Zhu, J., Xu, X., and Huang, Z.: Active fault survey and earthquake hazard assessment in Fuzhou, Science Press, https://doi.org/10.3969/j.issn.1001-4683.2005.01.001, 2005 (in Chinese).

Zhang, P., Deng, Q., Zhang, G., Ma, J., Gan, W., Min, W., Mao, F., and Wang, Q.: Active tectonic blocks and strong earthquakes in the continent of China, Sci. China Ser. D, 46(2), 13-24, 2003.